

AFOSR TR-80-0582

18

19

LEVEL

13

6

MEASUREMENTS OF THE EFFECTS OF SHOCK PRESSURE ON
TWO INSULATORS: AgI AND KAPTON,

DDC FILE COPY
AUG 81 12

9) Final Report. 1 Jan 78 - 30 Jun 80

15) AFOSR-78-3478

16) 2306

17) AI

10) by G. E. Duvall and E. R. Lemar

Washington State University
Department of Physics
Pullman, WA 99164

DTIC
ELECTE
AUG 15 1980
S C D

Research sponsored by the Air Force Office of Scientific Research, Air Force Systems Command, USAF, under Grant No. AFOSR 78-3478. The United States Government is authorized to reproduce and distribute reprints for Governmental purposes notwithstanding any copyright notations hereon.

Approved for public release; distribution unlimited.

11) Jul 1980

12) 51

80 8 14

1/01959
105

DDC FILE COPY

UNCLASSIFIED

SECURITY CLASSIFICATION OF THIS PAGE (When Date Entered)

REPORT DOCUMENTATION PAGE		READ INSTRUCTIONS BEFORE COMPLETING FORM
1. REPORT NUMBER AFOSR-TR- 80-0582	2. GOVT ACCESSION NO. AD-A088112	3. RECIPIENT'S CATALOG NUMBER
4. TITLE (and Subtitle) Measurements of the Effects of Shock Pressure on Two Insulators: AgI and Kapton		5. TYPE OF REPORT & PERIOD COVERED Final Report 1/1/78 - 6/30/80
7. AUTHOR(s) G. E. Duvall and E. R. Lemar		6. PERFORMING ORG. REPORT NUMBER
9. PERFORMING ORGANIZATION NAME AND ADDRESS Washington State University Department of Physics Pullman, WA 99164		8. CONTRACT OR GRANT NUMBER(s) AFOSR 78-3478 <i>rel</i>
11. CONTROLLING OFFICE NAME AND ADDRESS Air Force Office of Scientific Research Bolling AFB Washington, D.C. 20332		10. PROGRAM ELEMENT, PROJECT, TASK AREA & WORK UNIT NUMBERS 2306/A1 <i>6.110.24</i>
14. MONITORING AGENCY NAME & ADDRESS (if different from Controlling Office)		12. REPORT DATE 7/7/80
		13. NUMBER OF PAGES 46
		15. SECURITY CLASS. (of this report) unclassified
		15a. DECLASSIFICATION/DOWNGRADING SCHEDULE
16. DISTRIBUTION STATEMENT (of this Report) Approved for public release; distribution unlimited		
17. DISTRIBUTION STATEMENT (of the abstract entered in Block 20, if different from Report)		
18. SUPPLEMENTARY NOTES		
19. KEY WORDS (Continue on reverse side if necessary and identify by block number) Silver Iodide Resistivity Pressure Shock Waves Conductivity Kapton		
20. ABSTRACT (Continue on reverse side if necessary and identify by block number) The electrical conductivity of AgI has been measured at pressures between 7.79 and 40.9 kbar. Thin disk-shaped samples were prepared by pressing 99.99% pure AgI powder at 4 kbars for three hours. The samples were impacted in a gas gun, and the resistance was measured between electrodes that had been vacuum deposited on the front and rear surfaces of the samples. The data from these experiments are characterized by a rapid decrease in resistance as the shock wave reaches the front electrode, followed by a		

DD FORM 1 JAN 75 1473

EDITION OF 1 NOV 65 IS OBSOLETE
S/N 0102-LF-014-6601

UNCLASSIFIED
SECURITY CLASSIFICATION OF THIS PAGE (When Date Entered)

UNCLASSIFIED

SECURITY CLASSIFICATION OF THIS PAGE(When Data Entered)

further decrease as the shock wave travels through the sample and rear electrode into a backing plate of AgI. The resistance reaches a steady value several μsec after the shock wave has traversed the sample and while the sample is still in a state of steady pressure. The steady value of resistivity decreases with increasing pressure.

Resistances of Kapton films 1.05 and 3.05×10^{-3} inches thick have been measured with the film compressed between two copper plates. Pressures ranged from 40 to 150 kbars. Resistivity decreased in two steps by 10 to 12 orders of magnitude; final resistivity decreases monotonically with increasing pressure. The results are in general agreement with Graham's model of bond scission in polymers, and there is some suggestion of separate contributions by surface and volume effects to the final resistivity.

Accession For

NTIS GRA&I

DDC TAB

Unannounced

Justification

By _____

Distribution/ _____

Availability Codes

Dist	Avail and/or special
A	

UNCLASSIFIED

SECURITY CLASSIFICATION OF THIS PAGE(When Data Entered)

TABLE OF CONTENTS

	Page
PART I: Electrical Conductivity of Shock-Compressed AgI, E. R. Lemar and G. E. Duvall	
INTRODUCTION	1
EXPERIMENTAL DESIGN	2
Sample Preparation	2
Target Preparation	4
Projectile Design	5
Resistance Measuring Circuit	5
x-t Diagram	8
AgI Hugoniot	10
PMMA Hugoniot	10
EXPERIMENTAL RESULTS	11
General Observations	11
Shock Wave Data	13
DISCUSSION	18
REFERENCES to Part I	23
 PART II: Electrical Conductivity of Shock-Compressed Kapton Polyimide Films, E. R. Lemar	
INTRODUCTION	25
EXPERIMENTAL DESIGN	25
Target Preparation	25
Projectile Design	27
Resistance Measuring Circuit	27
Ringing up to Pressure	30
Resistivity	33
EXPERIMENTAL RESULTS	36
Response Time	36
Resistivity Data	45
REFERENCES to Part II	46

AIR FORCE OFFICE OF SCIENTIFIC RESEARCH (AFSC)
 NOTICE OF TRANSMITTAL TO DDC
 This technical report has been reviewed and is
 approved for public release IAW AFR 190-12 (7b).
 Distribution is unlimited.
 A. D. BLOSE
 Technical Information Officer

PART I

ELECTRICAL CONDUCTIVITY OF SHOCK-COMPRESSED AgI

E. R. Lemar and G. E. Duvall

INTRODUCTION

In this set of experiments we are studying the electrical conductivity of AgI under conditions of shock wave compression. Samples are impacted in a 4 inch diameter light gas gun and the resistance is measured during and after the shock wave passage through the material.

In a material there can be both electronic and ionic conduction taking place. In electronic conduction, electrons travel from one electrode to the other to form the current. In ionic conduction, ions of the material form the current. In general a material may exhibit both electronic and ionic conductivity simultaneously, making the interpretation of data difficult.

Silver iodide was chosen for these experiments since, at least at atmospheric pressure, it exhibits only ionic conductivity. In addition, it is readily available, and a great deal of static high pressure work has been done on the material allowing us to compare our work with that of others. One disadvantage is that large single crystals of AgI cannot be grown, which forces us to work with polycrystalline samples.

The main problem encountered in performing conductivity measurements on ionic conductors is obtaining good electrodes. The electrodes must be in intimate contact with the sample so that ions can leave the electrodes and enter the sample. Silver ions are the charge carriers in AgI, so vapor plated silver electrodes were used. Even vapor plating does not yield good electrodes for conductivity measurements at atmospheric pressure. In our experiments, measurements of the sample resistances at atmospheric pressure prior to a shot were from 2 to 600 times too large, indicating very poor contact between the electrode and the AgI. When the shock wave traverses the electrode, the electrode does become very good. An extrapolation of our data back to zero pressure gives a conductivity that is in good agreement with that given by Schock and Katz.¹ They obtained their atmospheric pressure value after precompressing the sample to high pressure.

Even with a good electrode, only a small fraction of the electrode material is in good contact with the sample. The electrode resistance will increase as the current flows through the sample depleting the portion of the electrode that is in good contact. Thus AC should be used for the resistance measurements. Then the electrodes are being continually depleted and replenished. Due to the short length of time that the sample remains at pressure during a shock experiment, AC measurements are difficult to make. However, if the DC current is turned on just prior to the shock wave arrival, and the experiment lasts for only a few microseconds, no more current flows through the sample than during half a cycle of a high frequency AC measurement. In these experiments we have done just that, so our measurements are equivalent to high frequency AC measurements.

In conclusion, resistance measurements on ionic conductors like AgI can be difficult, but the problems are not insurmountable. Some care must be taken, however, in interpreting the various data taken by ourselves and others, and we must realize that the data can be greatly affected by contact resistance.

EXPERIMENTAL DESIGN

The AgI target assembly used in these experiments is shown in Fig. 1. It consists of a thin polymethylmethacrylate (PMMA) buffer plate on to which our AgI sample has been epoxied. A backing plate of AgI is epoxied on the rear surface of the sample. The buffer plate is impacted and the resulting shock wave travels through the sample and into the backing plate. The purpose of the buffer plate is to protect the front electrode of the sample during target preparation. It was also felt that the front electrode might suffer damage if it were impacted directly.

Sample Preparation

The samples were prepared from 99.99% pure AgI obtained from Hudson Laboratories.² The initial batch of AgI was found to contain substantial quantities of water, so all of the material used in these experiments was first dried by placing it in a

Silver Iodide Sample

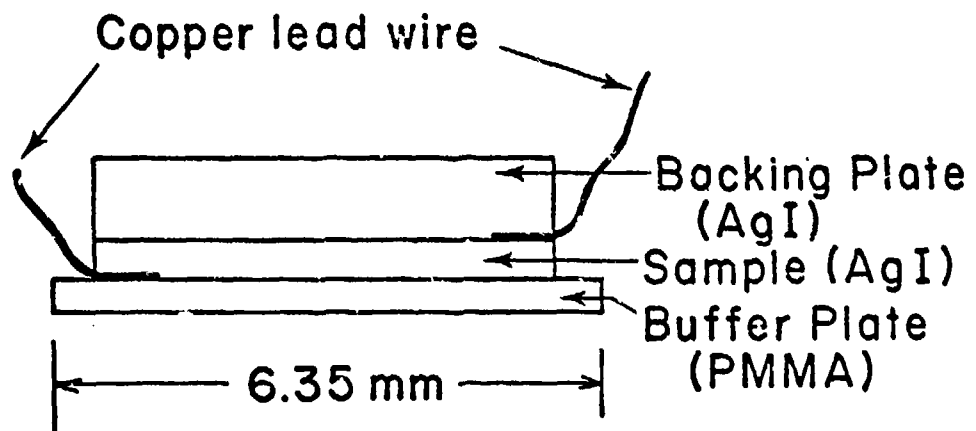
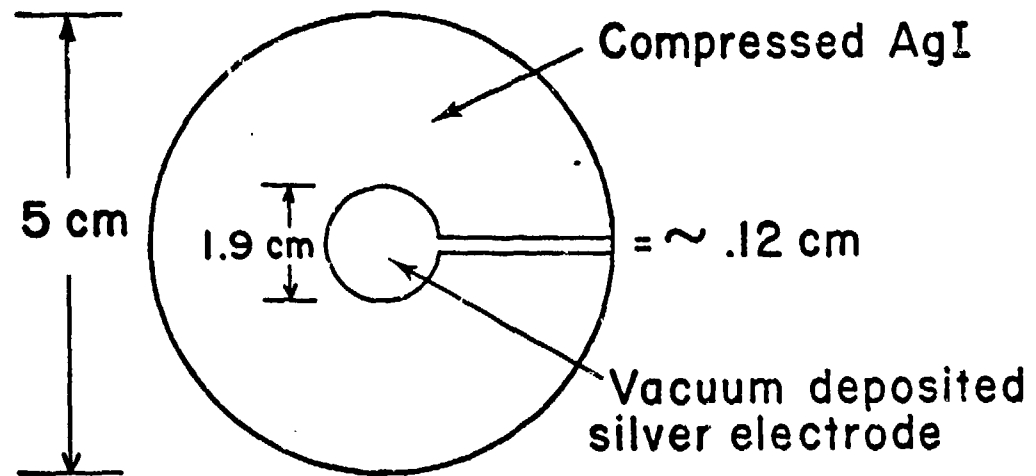


Figure 1. AgI target assembly.

vacuum desiccator and pumping on it for several days. The AgI was then stored either under vacuum or in a desiccator with a drying agent until used.

To prepare a sample the required amount of AgI powder was re-ground in a glass mortar and pestle. The powder was then loaded into a piston and cylinder-shaped die. The die was designed so that a vacuum could be pulled on the powder prior to pressing. The loaded die was then placed in a hydraulic press and the sample was brought up to 2.2 kbar and kept at that pressure for 3 hours. The resulting samples had densities that were about 95% crystal density and showed some brown discoloration. This discoloration has been reported by various authors^{3,4} and is probably due to a decomposition of some of the material into Ag and I. It is not a surface effect but extends completely through the samples. No attempts were made to get higher densities by heating the samples while they were being pressed, since Allen and Lazarus⁴ have reported that heating the die produces contaminated samples that turn black with exposure to light.

Target Preparation

The two surfaces of the thin disk-shaped samples were then sanded flat and parallel to each other within a few microns over the whole two-inch diameter of the disks. No lubricant was used on the sandpaper since this would contaminate the surface and make good electrical contact difficult to achieve. A brass mask was placed on the sample and a one micron thick silver electrode was vacuum deposited on each of the two flat surfaces. A short piece of #26 bare copper wire was attached to each of the electrodes with silver conductive paint. The joint between the electrode and the wire was then covered with Devcon 5 Minute Epoxy to give it more strength. A thin buffer plate of PMMA was epoxied over the silver electrode on the impact surface of the sample, and a AgI backing plate was epoxied over the electrode on the rear surface. The epoxy bonds are only 2 or 3 microns thick so they have little effect on the shock traversing the assembly. The sample was then potted in epoxy in a target holder for mounting in the gun.

Projectile Design

Standard aluminum projectiles were used for all but one of the AgI experiments. The impact surface of the projectile (Fig. 2) had a hole recessed in it and a PMMA impactor was epoxied in the hole. The impact surface was then lapped flat and perpendicular to the axis of the projectile. The collar of aluminum outside the impactor was used to short a pin to trigger the scopes.

A brass ring was epoxied in a recess around the edge of the PMMA impactor and used to close the switch that applied the capacitor voltage to the sample. This brass ring was electrically isolated from the aluminum projectile. For the highest velocity shot the aluminum projectiles were too heavy, so a nylon encased syntactic foam projectile with a PMMA impactor was used.

Resistance Measuring Circuit

The resistance measuring circuit (Fig. 3) consists of a capacitor that is charged to 15 V through a 100 k Ω resistor and discharged through the sample and a resistor in series with it when the switch is closed by the projectile at impact. The entire circuit is built on the back of each target in order to minimize the lead length and thus maximize the frequency response. The capacitor is a standard 100 μ f, 25 VDC electrolytic capacitor. Since it must operate in a vacuum, it is sealed by potting it in epoxy. The capacitance is so large that the voltage across the capacitor is constant to a fraction of a percent for the 10 μ sec duration of the experiment. It is interesting to note that since the switch is closed only about 0.3 μ sec before the shock enters the AgI, and the experiment lasts for about 10 μ sec, these DC measurements are equivalent to measurements taken with a 50 kHz square wave.

An analysis of the circuit shows that the resistance of the sample R_s is given by the following expression after the switch has been closed.

$$R_s = [RZ_L / (R + Z_L)] [(V_o / V_L) - 1]$$

Projectile Impact Surface

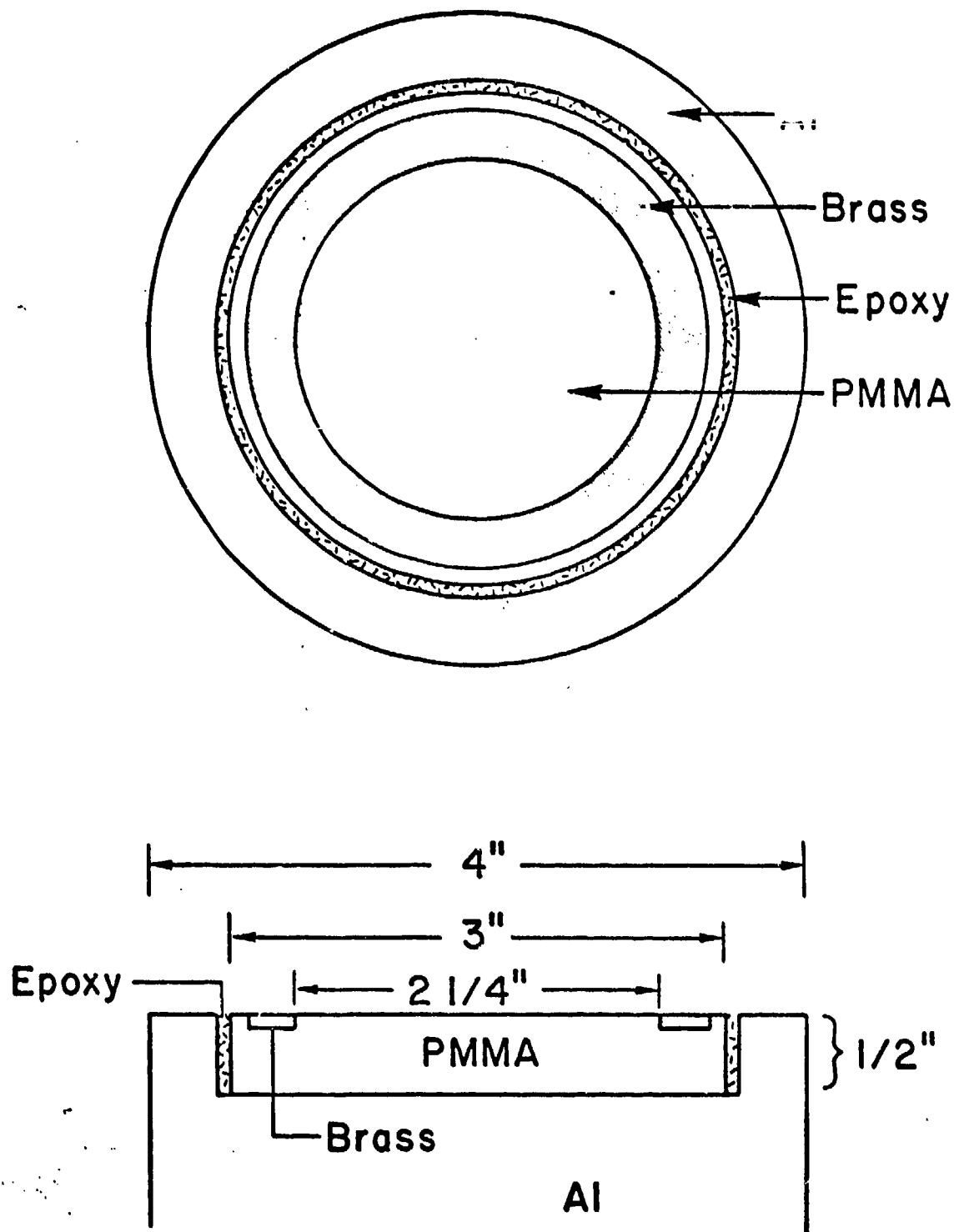
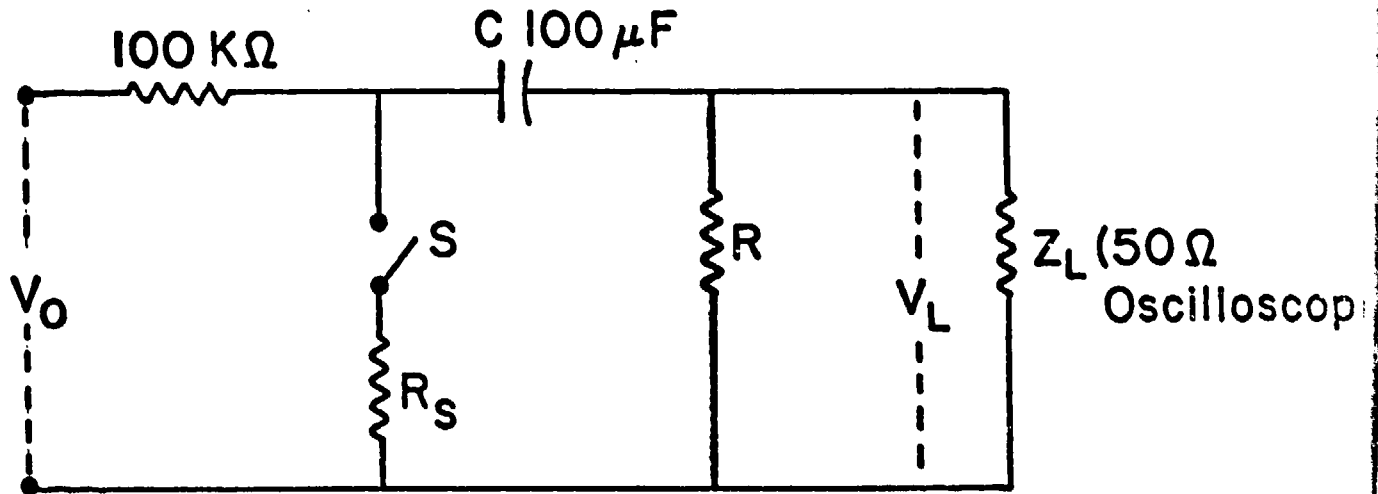


Figure 2. Projectile impact face.

Resistance Measurement Circuit



R_S Ag I sample

V_L voltage measured by the oscilloscope

When the switch is closed

$$R_S = \frac{R Z_L}{R + Z_L} \left[\frac{V_0}{V_L} - 1 \right]$$

This is of the form

$$R_S = \frac{A}{V_L} + B$$

Figure 3. Resistance measurement circuit.

This expression is of the form

$$R_s = AV^{-1} + B$$

where A and B are constants. Before each shot the sample and switch are replaced in the circuit by known resistors and a mercury relay. This allows us to calibrate the scopes by measuring the deflections given by several known resistors. The constants A and B are then determined with a linear least squares fitting program.

x-t Diagram

A generalized x-t diagram for the present series of resistance experiments is shown in Fig. 4. When the PMMA impactor in the projectile strikes the PMMA buffer plate on the sample, a shock wave is sent into the impactor and into the buffer plate. When the shock in the buffer plate reaches the AgI, a shock is sent into the AgI and one is reflected back into the buffer plate. Since the buffer plate and the impactor are of the same material, the interface between the two does not exist after impact, and this wave continues back into the impactor with no reflection at this point. The shock wave in the sample continues into the backing plate of AgI with no reflection at the interface between the two. The sample is now in a state of steady pressure and will remain so until the waves reflecting off the far surfaces of the impactor or the backing plate get back to the sample. The electrodes are located in the centers of the sample surfaces so that the lateral rarefactions do not enter the active area of the sample during data gathering.

In these experiments, the samples were about 50 mm in diameter and from 2.5 to 3 mm thick. The silver electrodes were about 19 mm in diameter. The PMMA impactors were about 12 mm thick for all but the first three shots, where they were only about 6 mm thick. The PMMA buffer plates were about 1 to 1.25 mm thick, and the AgI backing plates were about 5 mm thick. With these dimensions, the samples were at constant pressure for about 5 μ sec.

9

Sample is at steady pressure

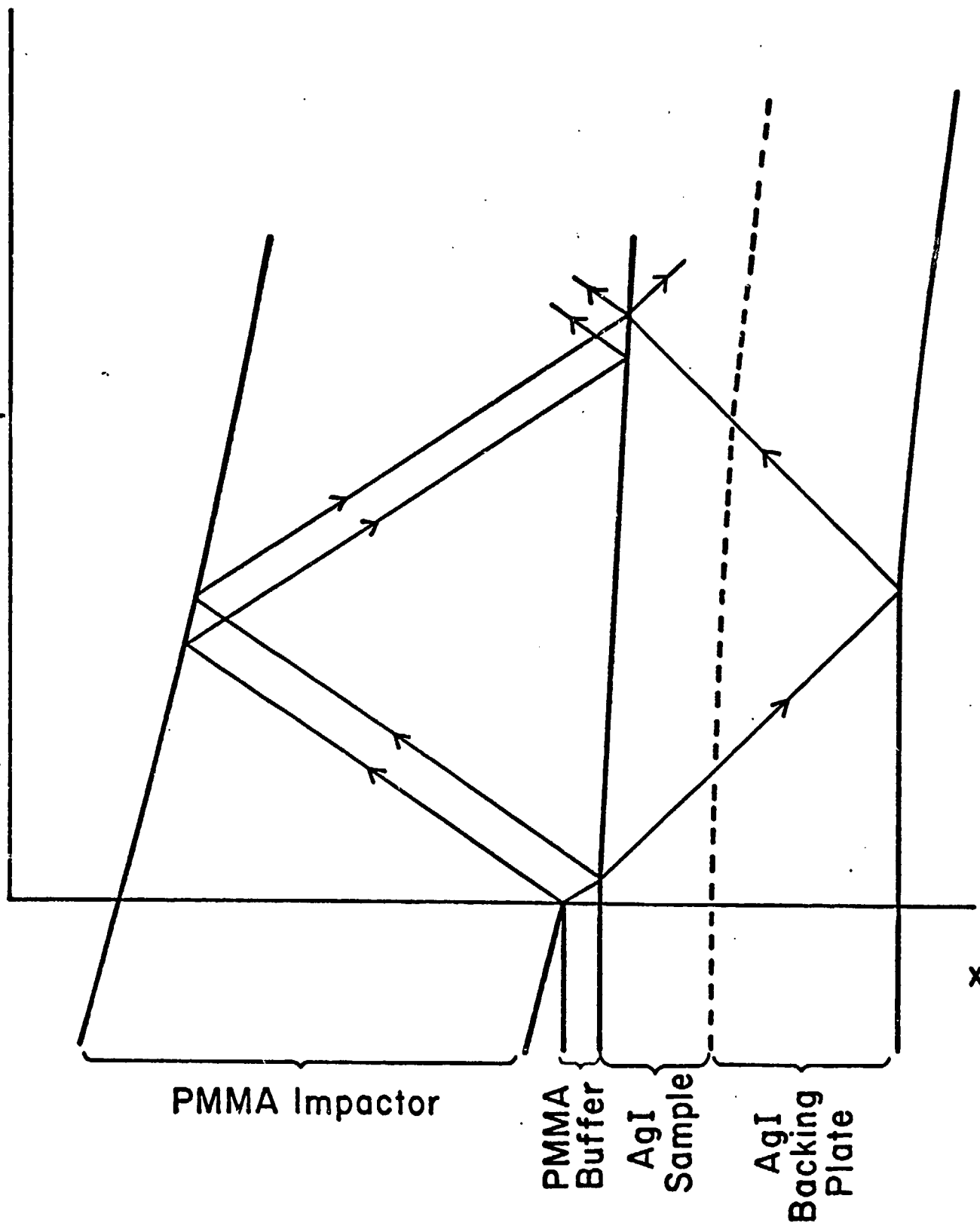


Figure 9. x-t Diagram.

AgI Hugoniot

In order to determine the pressure in the shocked samples, the Hugoniot curve for AgI must be known. Since no published data could be found, an approximation for the Hugoniot was determined by measuring the longitudinal and transverse sound speeds in a compressed AgI sample. The longitudinal sound speed c_L is 2.224 mm/ μ sec, and the transverse sound speed c_T is 0.878 mm/ μ sec. From these we can obtain the bulk sound speed c_0 .

$$c_0 = (c_L^2 - \frac{4}{3} c_T^2)^{1/2}$$

$$= 1.979 \text{ mm}/\mu\text{sec}$$

The density ρ_0 of AgI is 5.683 g/cm³. A linear approximation to the Hugoniot is then given by

$$P = \rho_0 c_0 u_p$$

where u_p is the particle velocity in mm/ μ sec. Thus we have

$$P \text{ (kbar)} = 112.5 u_p.$$

The potential for improving this Hugoniot does exist in our resistance data. On a number of the oscilloscope photographs, the shock wave arrival times at the front and rear electrodes of the sample can be determined. This gives the shock velocity, from which we can obtain the Hugoniot, since we do know the Hugoniot of the impactor and buffer plate material. This has not been done in any systematic manner yet, but there are indications that our linear approximation to the Hugoniot may be 5 to 10% too low. The main difficulty in obtaining the shock velocity from our data is that the sweep time needed to record the resistance data is too long to give an extremely accurate measurement of the much shorter shock transit time.

PMMA Hugoniot

The PMMA used in these experiments was either Rohm and Haas Plexiglas II UVA or Rohm and Haas Plexiglas. For the first three shots, 6 mm thick impactors of

II UVA were used and the buffer plates were of the same material. The results of these shots showed that we needed to have the sample remain at pressure for a longer time. This necessitated the use of 12 mm thick impactors. Since no II UVA of this thickness was available in the laboratory, regular Plexiglas was used for the rest of the shots. The buffer plates on these remaining shots were also regular Plexiglas.

The Hugoniot for PMMA is dependent on the manufacturer and probably the particular batch of material used. In our work the various Hugoniots give pressures that differ by a few percent. These differences are less than the uncertainty in our AgI Hugoniot. In this work we have used the following Hugoniot for PMMA:⁶

$$P = 11.86(2.598 + 1.516u_p)u_p.$$

The pressure P is in kbar and the particle velocity u_p is in mm/ μ sec.

EXPERIMENTAL RESULTS

General Observations

Before the shock resistance data is presented, some general observations should be made. The AgI used in these experiments came from four batches obtained from Hudson Laboratories. The first three batches were all 99.99% pure and the last batch, used only for backing plates for the last two shots, was 99.9+% pure by their analysis. The amount of discoloration in a compressed sample was dependent upon the particular batch of material used. The first and third batches discolored badly, while the second batch discolored much less. The fourth batch discolored much more than any of the others. When the samples were potted, the brown color diffused into the uncured epoxy. The amount of discoloration in the various batches may be related to the particle size in powdered AgI. Schock and Katz³ have observed that in a pressure gradient, AgI dissociates with the metal ions collecting irreversibly in the low-pressure area and halide ions collecting in the high-pressure areas, where they combine to form molecular iodine. The Ag^+ ions are then reduced

to silver by incident light. Larger particle size should give larger pressure gradients and yield more discoloration.

While the second batch did not stain as badly, it did stick to the steel die after pressing. This problem was solved by spraying the die with a release agent (Miller-Stephenson MS-122 Fluorocarbon Release Agent Dry Lubricant). The die was then cleaned by rubbing it with Kimwipes before a sample was pressed. Any possible surface contamination of the samples was removed when the samples were sanded.

None of the vacuum deposited silver electrodes used in these experiments were electrically very good at atmospheric pressure. The stained samples tended to form better electrodes than the unstained samples. However, all of our attempts to get meaningful and consistent atmospheric pressure resistivities were unsuccessful. When a DC voltage is applied to a sample, the resistance increases with time indicating that the small fraction of the electrode that is in good electrical contact is being depleted. Measurements taken with an AC bridge did not give values of resistivity that were consistent from sample to sample either. No significant change in a sample's resistance was detected as the frequency was varied from 1 kHz to 100 kHz. Attempts were made to obtain better electrodes by heating a sample after the electrodes had been deposited. The 1 kHz AC resistance of a sample was measured as it was heated in an argon atmosphere. As the sample was heated to 110°C, the resistance did decrease. However, after the sample had cooled to room temperature the resistance was greater than it had been prior to heating. When the same sample was heated to 160°C and then cooled, cracks developed and the sample increased in thickness by about 3%. At 146°C AgI undergoes a phase change to a more dense superionic conducting phase.⁵ Temperature cycling through this volume discontinuity produces cracks in the samples. This problem could possibly be alleviated by heating the sample under pressure. Since our electrodes are good after the shock wave passes through, no other attempts were made to obtain good electrodes at atmospheric pressure.

Shock Wave Data

Figure 5 shows resistivity versus time after shock wave arrival at the second electrode for three different projectile velocities. It should be noted that the resistivities reported have not been corrected for electrode edge effects, but identical electrodes were used for all the shots. After the shock wave has arrived at the second electrode, the whole sample remains in a state of steady pressure until waves reflected from the rear surface of the impactor or backing plate arrive at one of the electrodes. The resistivity, however, does not achieve a steady value until the sample has been at pressure for 1 to 4 μ sec. This steady value will be called the final resistivity. It is unclear whether this is an electrode effect or a property of the bulk material. This does necessitate a very long recording time for a shock experiment and required us to use 12 mm thick impactors. As the projectile velocity, and thus pressure, is increased, the final value of resistance is reached in a shorter period of time. On some of the shots the resistivity undershot the final value. The resistivity change at the end of the steady region is due to reflected waves arriving back at the electrodes and lateral rarefactions entering the region of the sample between the electrodes.

In all but one of the shots the applied current was in the direction of the shock wave. In the one shot (78-031) with the current applied in the opposite direction, there is a drop in resistance when the shock wave reaches the second (positive) electrode. This is shown as point A in Fig. 6 where we plot resistivity versus time for shots 78-031 and 78-027. These two shots on Batch I AgI at about the same velocity give data that agree very well. The differences that occur before the shock wave arrives at the second electrode are due to a difference in thickness for the two samples.

The values of final resistivity gathered in our shots are presented in the table and Fig. 7. The pressure was determined by using the approximate AgI Hugoniot

Resistivity vs Time After Shock Wave
Arrival at Second Electrode

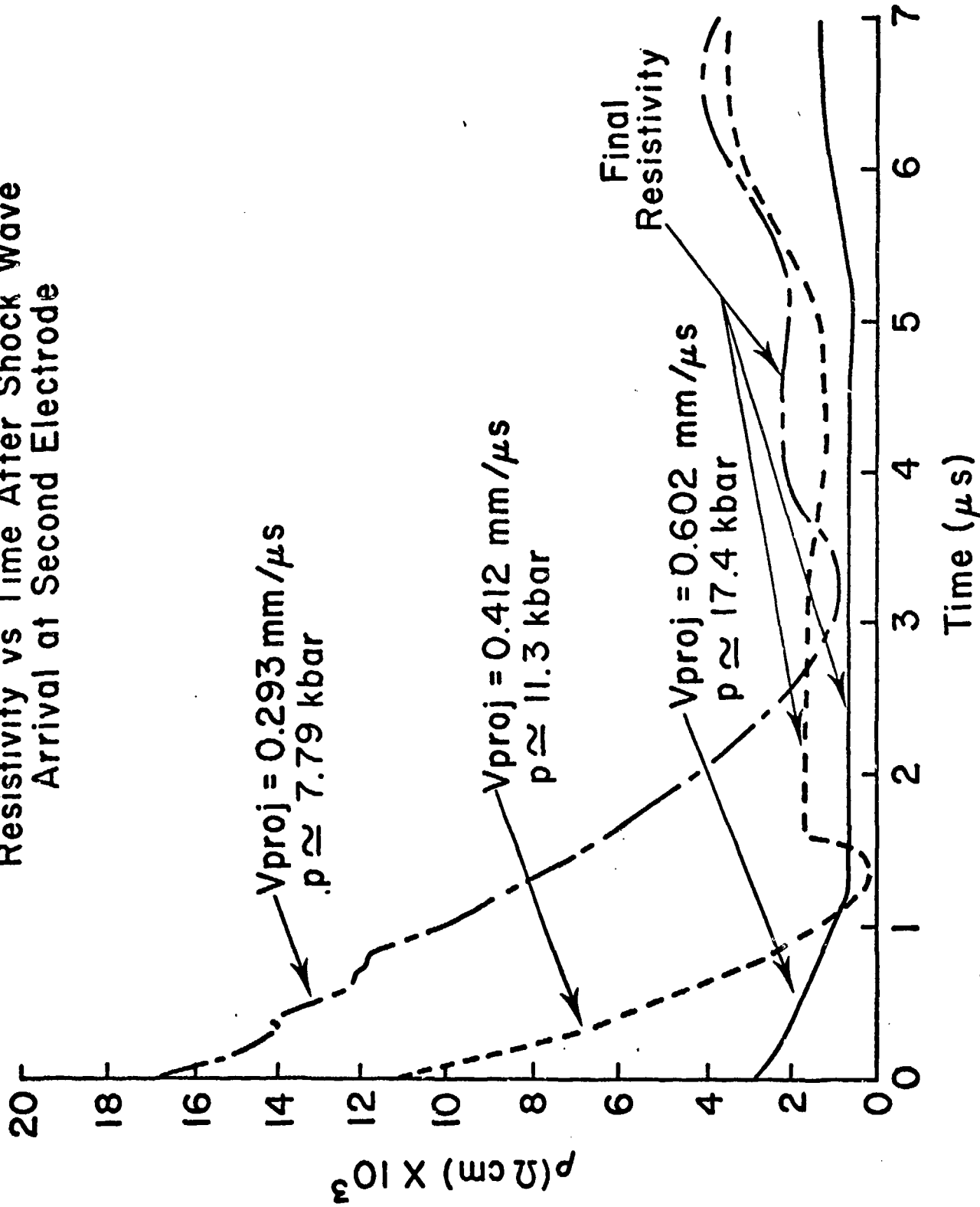


Figure 5. Resistivity versus time after shock wave arrival at second electrode.

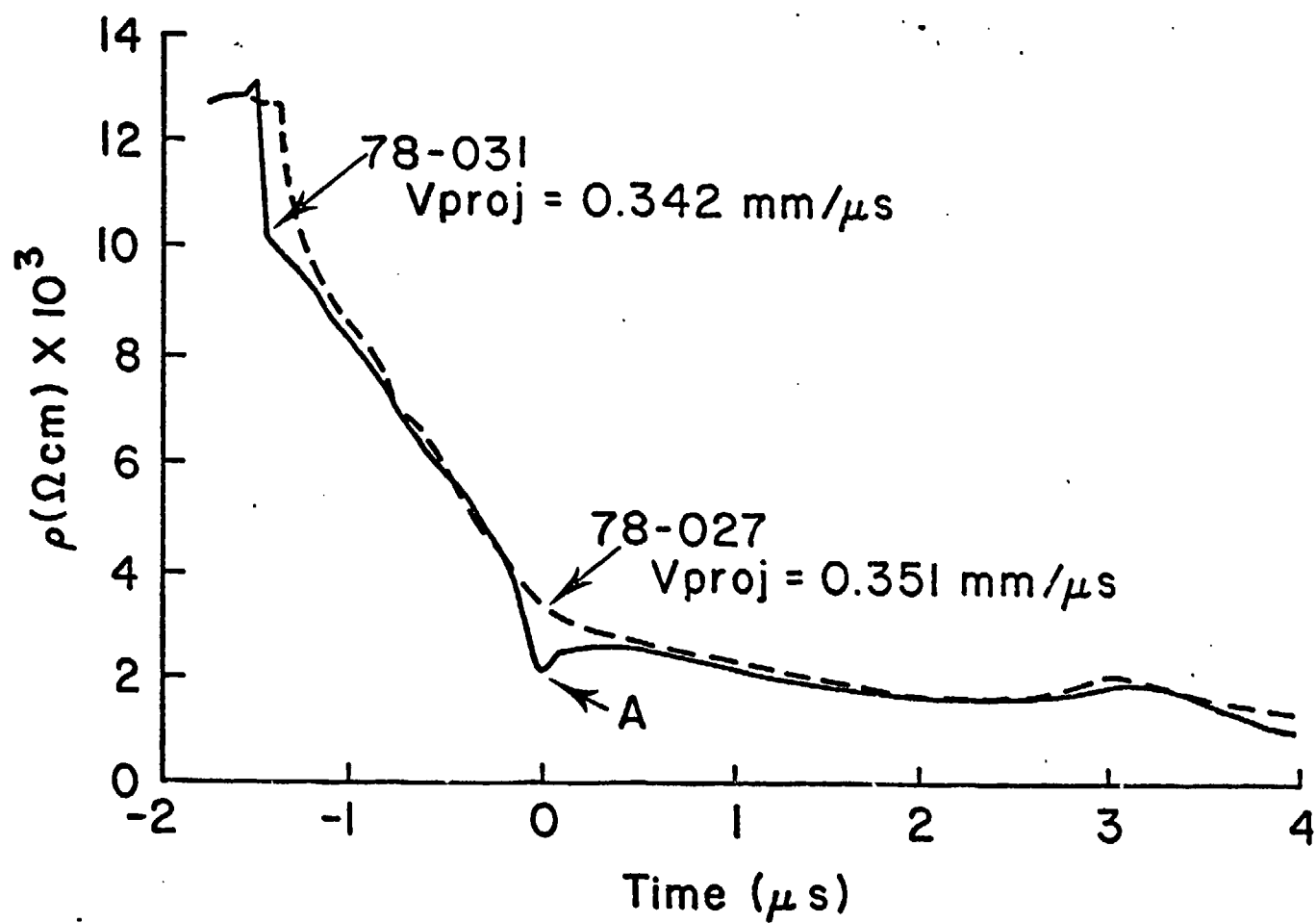


Figure 6. Resistivity versus time for shots 78-027 and 78-031.

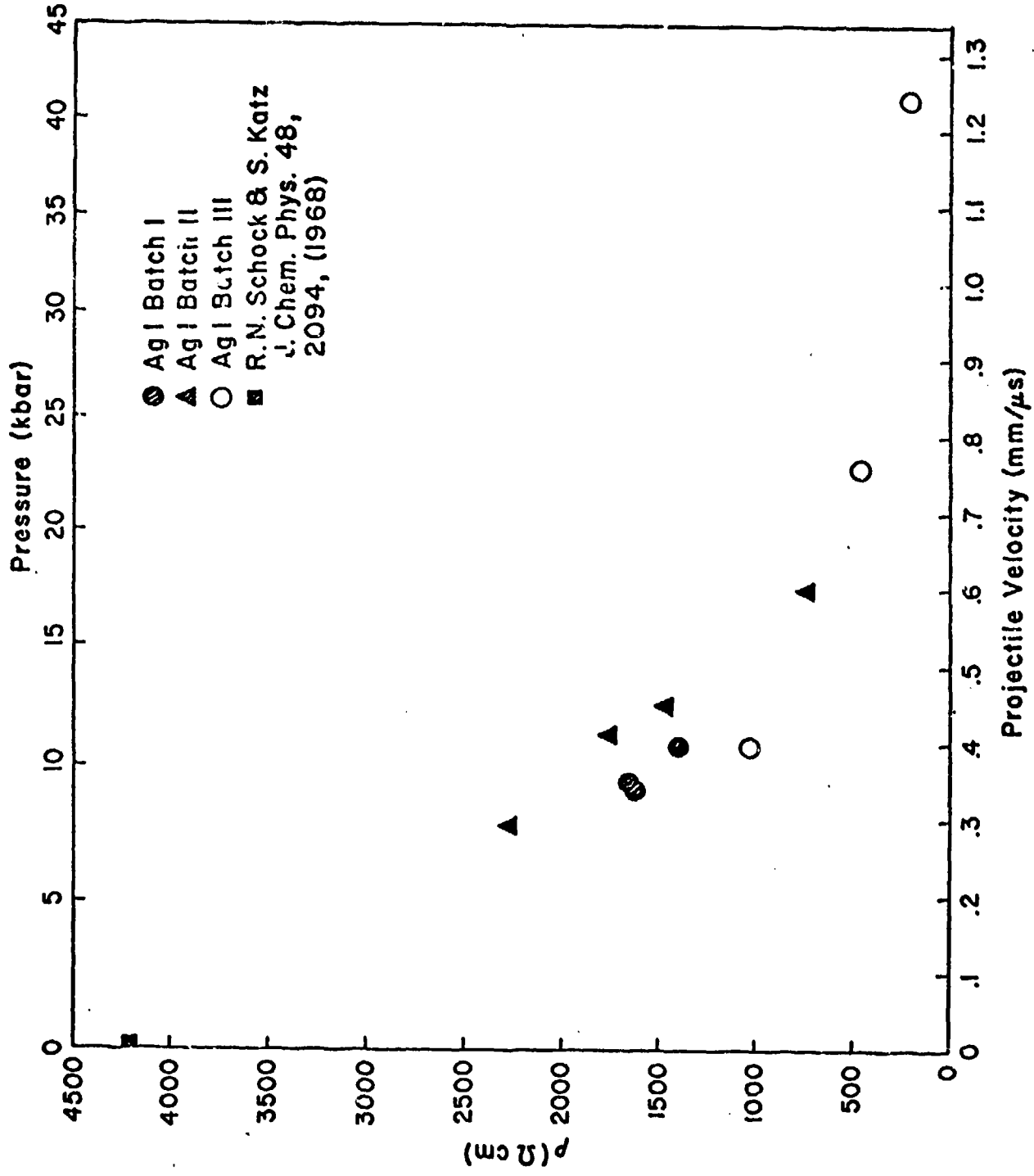


Figure 7. Resistivity versus projectile velocity.

Table: Silver Iodide Shock Wave Experiments

Shot #	AgI Batch #	Impactor Material	Impactor Thickness (mm)	Sample Thickness (mm)	Projectile Velocity (mm/μsec)	Pressure (kbar)	Final Resistivity (Ωcm)	Calculated Temperature Rise (°C)
78-027	I	II-UVA	≈6	3.05	0.351	9.49	1.64×10^3	18.8
78-030	I	II UVA	≈6	2.123	0.398	10.9	1.42×10^3	21.8
78-031	I	II UVA	≈6	3.225	0.342	9.20	1.62×10^3	18.2
78-038	II	Plexiglas	≈12	2.475	0.452	12.6	1.47×10^3	25.4
78-039	II	Plexiglas	≈12	2.488	0.293	7.79	2.25×10^3	15.2
78-041	II	Plexiglas	≈12	2.435	0.412	11.3	1.74×10^3	22.7
78-045	II	Plexiglas	≈12	2.545	0.602	17.4	7.31×10^2	36.4
78-048	III	Plexiglas	≈12	2.495	0.760	22.8	4.7×10^2	49.6
78-051	III	Plexiglas	≈12	2.295	0.400	10.9	$*1.03 \times 10^3$	21.9
78-052	III	Plexiglas	≈12	2.525	1.242	40.9	2.01×10^2	101

* Leads broke, see text.

discussed earlier. Figure 7 shows that the resistivity does depend on the particular batch of AgI used. Batch I material gave a lower resistivity than Batch II material. The resistivity given by shot 78-051 (the lowest velocity shot on Batch III material) should be viewed with suspicion. There is a discontinuity in the resistivity record of this shot which is probably due to a damaged electrode lead wire joint. This problem occurred on none of the other shots. This break occurred at about the time that the final resistivity value was being established. The resistivity did undershoot the final value and may not have reached the true final value before the damage occurred. This point should be viewed as a lower limit on the final resistivity.

Our data show that up to a pressure of about 17 kbar, the resistivity of AgI decreases almost linearly with increasing pressure. When our data are extrapolated to atmospheric pressure, we obtain a value for the resistivity which is 12% lower than the value given by Schock and Katz.¹ Above 17 kbar, the rate of decrease in resistivity becomes less and the resistivity may be approaching an asymptotic value greater than zero.

DISCUSSION

In Fig. 8, our data are compared with those of Schock and Katz.¹ Their work was done in a piston type high pressure cell. In their cell there was no direct relationship between the load force and the resulting pressure. Their pressure is known only at the points shown on the top scale. Thus a direct comparison between their data and our data is not possible. However, we can see that their conductivity decreases with pressure while ours increases. For the first few kilobars, their conductivity does increase with pressure, the rate of increase that they measure in this region seems to be greater than the rate that we have measured.

Riggleman and Drickamer⁷ have measured the resistance of AgI from 20 to 280 kbar. Their data show a decrease in resistance as the pressure is increased to 97 kbar. They attribute this decrease to an increase in electronic conduction. While

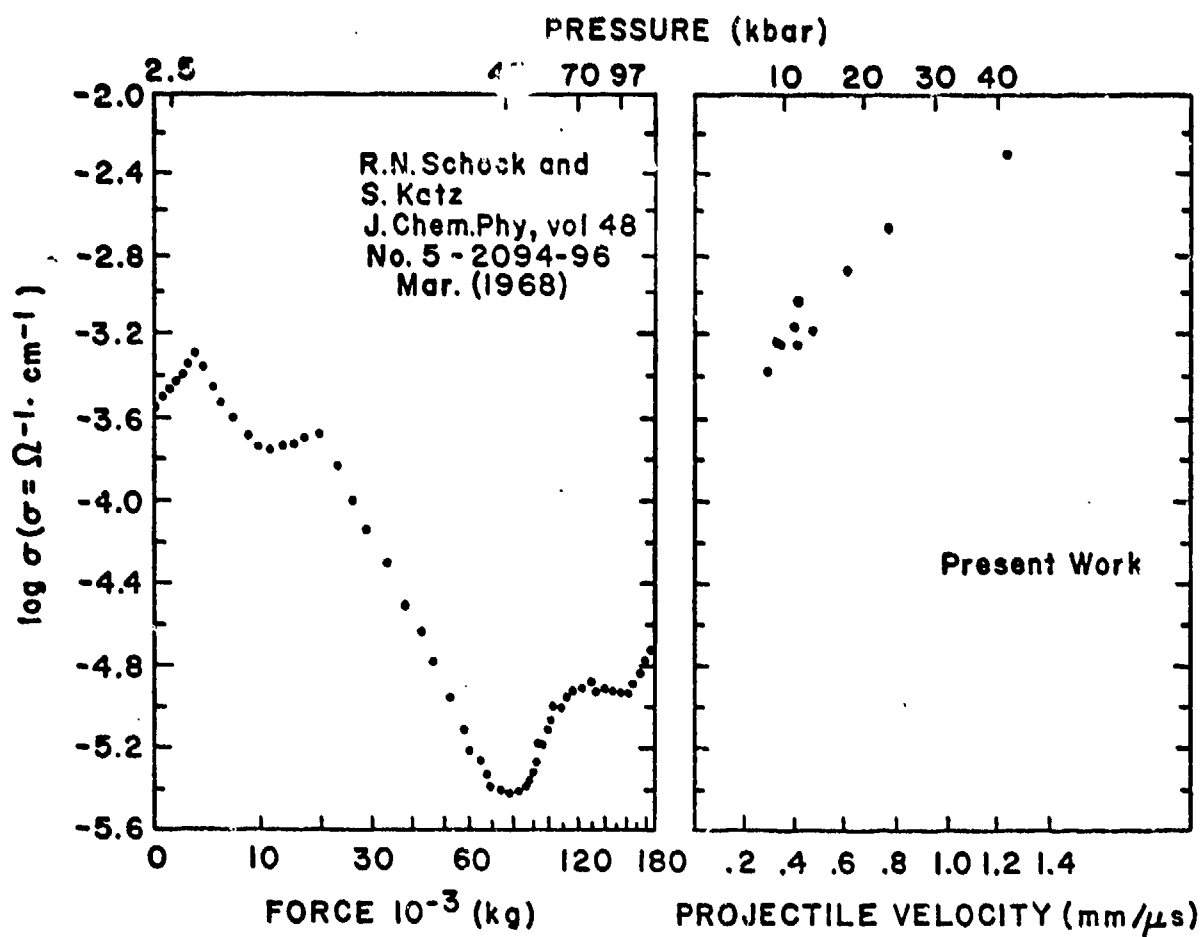


Figure 8. Log σ versus pressure.

our data is in qualitative agreement with theirs, our rate of decrease with pressure is much greater than theirs.

There is one obvious difference between a static high pressure experiment and a shock experiment. In a shock experiment we get not only an increase in pressure but also an increase in temperature as the shock wave traverses the sample. For a normal material shocked to these pressures, the increase in temperature is negligible. However, we are dealing with a porous solid. The work used in bringing the material up to full density goes into heating the material. The rise in temperature can be approximated in the following way.

Let T' = temperature of a porous material shocked to a pressure P
 T = temperature of a non-porous material shocked to a pressure P
 V'_0 = initial specific volume of a porous material
 V_0 = initial specific volume of a non-porous material
 V = final volume of either material

Then

$$\Delta T = T' - T \approx \left(\frac{\partial T}{\partial E}\right)_P (E' - E)$$

where

$$E' = \frac{1}{2}P(V'_0 - V)$$

$$E = \frac{1}{2}P(V_0 - V)$$

and

$$\left(\frac{\partial E}{\partial T}\right)_P = C_p - P\alpha V$$

Combining these we obtain

$$\Delta T \approx \frac{\frac{1}{2}P(V'_0 - V_0)}{C_p - P\alpha V}$$

If we choose

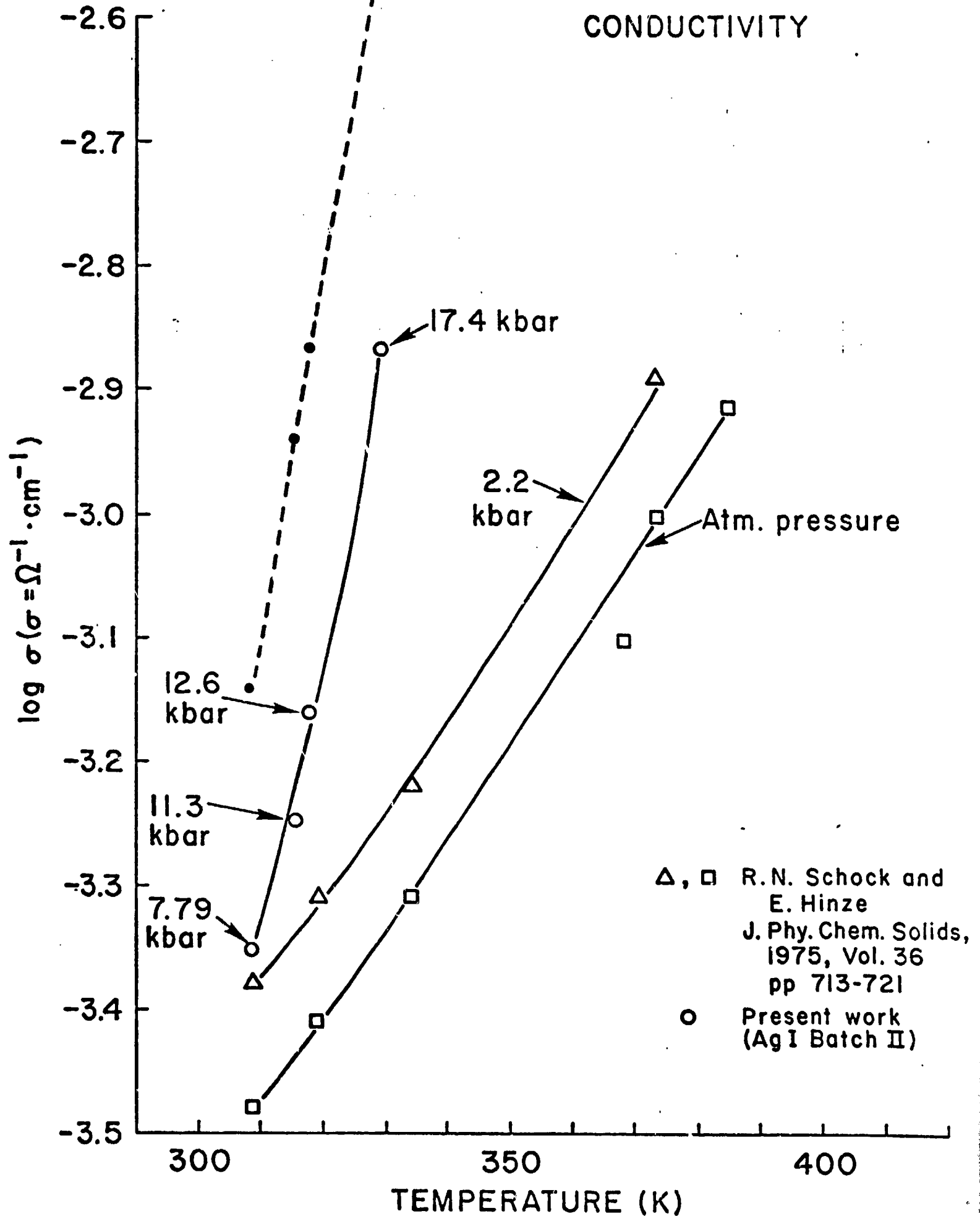
$$C_p = \text{constant} = 0.057 \text{ cal/gram degree} \quad (\text{average value between } 0 \text{ and } 100^\circ\text{C, Ref. 8})$$

$$\frac{V_0 - V}{V_0} = (4.11 \times 10^{-3})P, \quad P \text{ in kbar} \quad (\text{Ref. 8})$$

$$\alpha = 10^{-4} \quad (\text{an estimate based on other halides})$$

and a porosity of 5%, a 15 kbar shock will raise the temperature about 31°C. The temperature rise calculated for each shot is shown in the table.

In Fig. 9, our data for our Batch II AgI are plotted as a function of temperature. Some data of Schock and Hinze⁹ are presented on the same figure. Since their data go up to only a few kbar, a linear extrapolation of their data has been made to our high pressures. This extrapolation is given by the dotted line in the figure. The conductivities given by this extrapolation are about 1.8 times our values. Our Batch I material gave us conductivities that were about 1.3 times the conductivities given by the Batch II material that was plotted. Thus the differences between the dotted curve and our data are of the same order as the differences we obtain using various batches of AgI. Our higher pressure values do not agree, but a linear extrapolation of their data to 40 kbar should not be expected to give reasonable values.

SILVER IODIDE
CONDUCTIVITYFigure 9. $\log \sigma$ versus temperature.

REFERENCES

1. R. N. Schock and S. Katz, J. Chem. Phys. 48, 2094 (1968).
2. Hudson Laboratories, 410 S. Main St., Hudson, FL 33568.
3. R. N. Schock and S. Katz, J. Phys. Chem. Solids 28, 1985 (1967).
4. P. C. Allen and D. Lazarus, Phys. Rev. B 17, 1913 (1978).
5. Handbook of Chemistry and Physics (Chemical Rubber Co., Cleveland, 1967), 48th edition, pg. B-220.
6. "Selected Hugoniot," Los Alamos Scientific Laboratory Report LA-4167-MS, 1969.
7. B. M. Riggleman and H. G. Drickamer, J. Chem. Phys. 38, 2721 (1963).
8. Handbook of Physical Constants, edited by S. P. Clark, Jr., (The Geological Society of America, Inc., New York, 1966).
9. R. N. Schock and E. Hinze, J. Phys. Chem. Solids 36, 713 (1975).

PART II ;

ELECTRICAL CONDUCTIVITY OF SHOCK-COMPRESSED KAPTON POLYIMIDE FILMS

E. R. Lemar

INTRODUCTION

In these experiments we have studied the electrical conductivity of Dupont Kapton polyimide films under conditions of shock wave compression.

Kapton was chosen for these experiments since it is available in thin films and has been used as an insulator in shock work. In addition, Graham¹ has measured sizeable polarization signals from the bulk form of this material, showing that charge carriers are produced during shock compression.

These shots have been done on 1.05 and 3.05 mil thick samples at pressures from 39 to 152 kbar.

EXPERIMENTAL DESIGN

The Kapton target assembly used in these experiments is shown in Fig. 1. A thin film of aluminum plated Kapton is epoxied onto the back surface of a copper buffer plate. The buffer plate also serves as the front electrode. A smaller diameter copper disk is epoxied to the other side of the Kapton. It is used as the rear electrode.

Target Preparation

A 7.5 cm square sample of Kapton film was cleaned in ethyl alcohol and taped onto a polished brass plate. An aluminum film was then vapor deposited on the exposed surface.

The lapped and polished copper buffer plate with an attached lead wire was then epoxied to the sample that was still taped to the brass plate. When the epoxy had cured, the buffer plate and Kapton assembly were removed from the brass plate and placed in a mask that exposed a 2.557 cm diameter circular area of the back surface of the Kapton. This circular area was then vacuum deposited with aluminum. A 2.557 cm diameter lapped and polished copper electrode with an attached lead wire was then centered on the aluminized circle and epoxied in place.

Kapton Sample Assembly

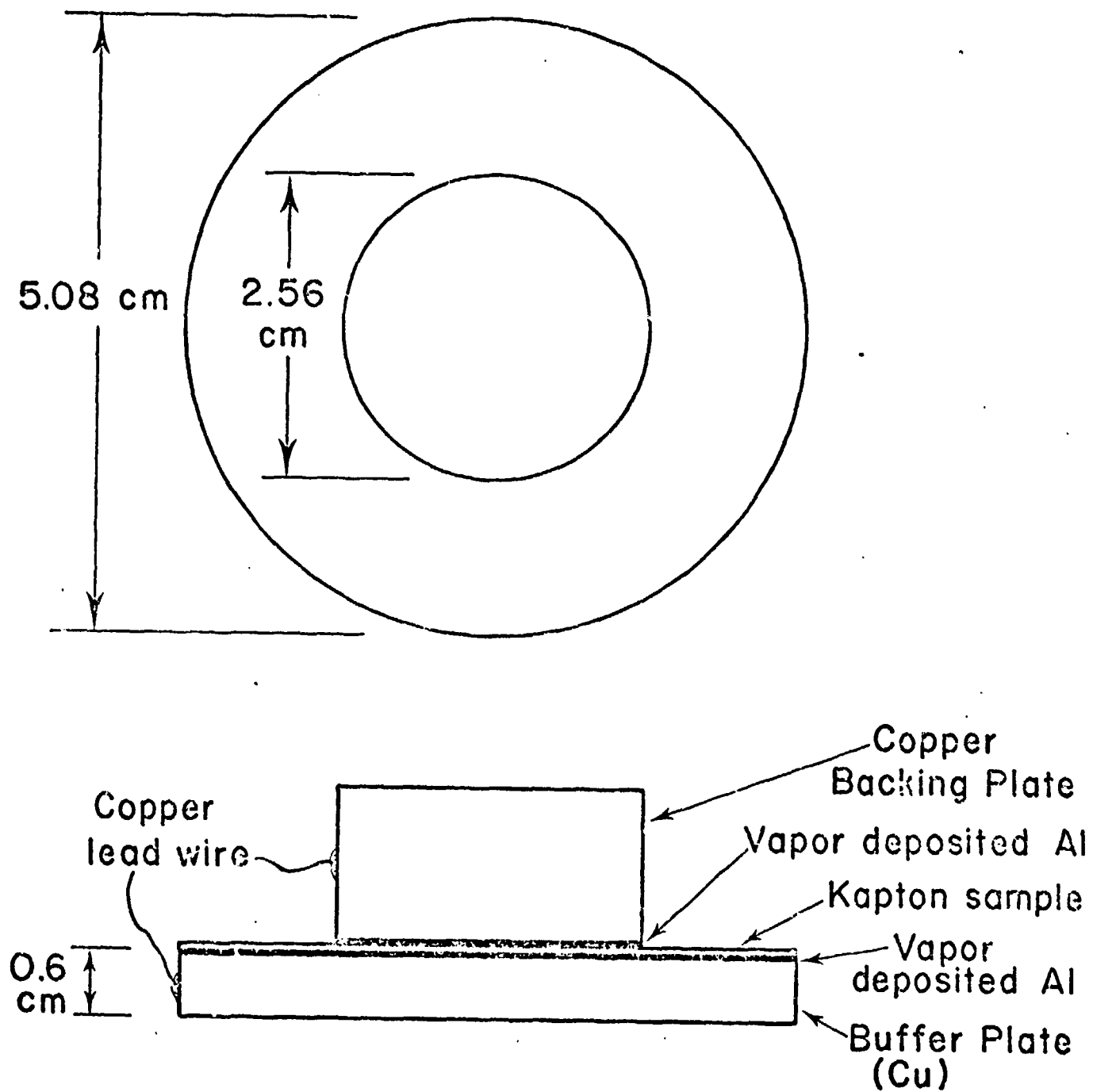


Fig. 1

The edges of this disk were rounded slightly to keep the Kapton from punching through when the shock wave arrived.

The plating of the Kapton was done to ensure that we had good electrodes on the Kapton. When the film of Kapton is epoxied to a polished copper plate, the irregularities in the surfaces prevent perfect contact between the two materials. In certain areas several microns of electrically insulating epoxy are left between the two materials. In other areas they touch. This could give large unpredictable contact resistance between the copper and the Kapton. Since the aluminum is vapor plated directly on the Kapton, it does make good contact on the whole area. Since copper and aluminum are both conductors, we do not need perfect contact to give us low contact resistance. Tests showed that the resistance between the copper plates and the aluminum films was just a small fraction of an ohm. Since the resistance of the shocked Kapton is still hundreds of ohms or larger, this contact resistance is negligible.

The sample was then potted in epoxy in a target holder for mounting in the gun.

Projectile Design

Standard aluminum projectiles were used for all of the Kapton resistivity shots. The impact surface of the projectile (Fig. 2) had a hole in it. A 2 cm thick copper impactor was epoxied in the hole. The impactor was electrically isolated from the body of the aluminum projectile.

Resistance Measuring Circuit

The resistance measuring circuit (Fig. 3) consisted of a 150 μ f, 50 V DC capacitor that was charged to 47.5 V through a 47 K Ω resistor and discharged through a series circuit of the sample, a 1 K Ω resistor, and a 50 Ω oscilloscope. The buffer plate electrode was the negative electrode.

This circuit was mounted on the back of the target. Since the capacitor must operate in the vacuum of the target chamber, it was sealed in epoxy. The

Projectile Impact Surface

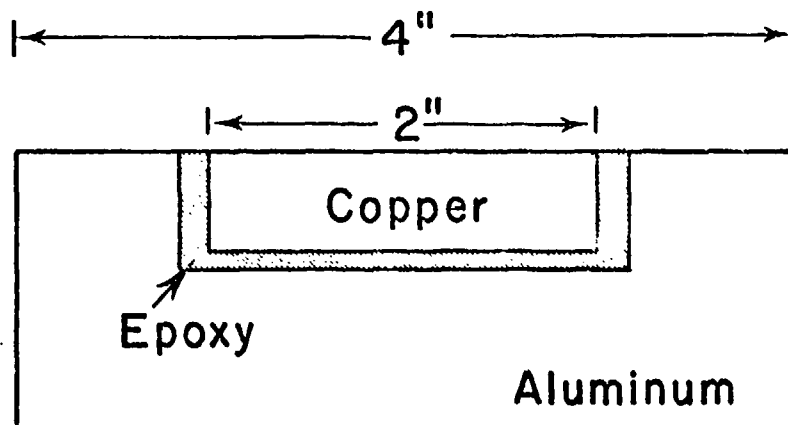
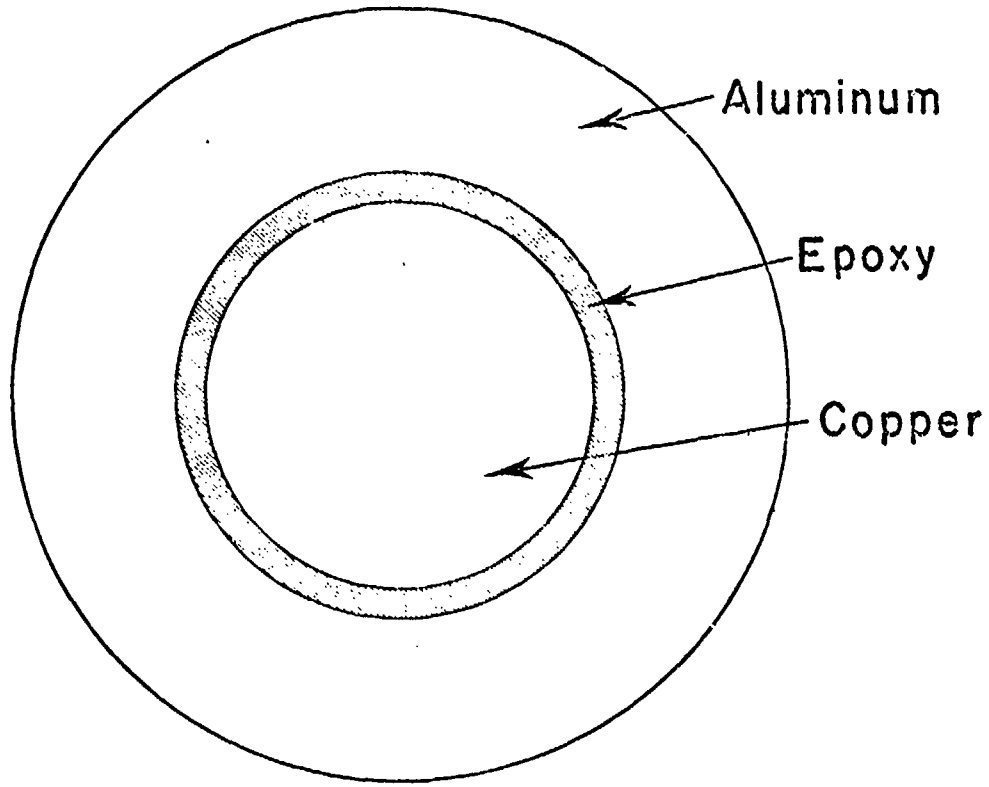
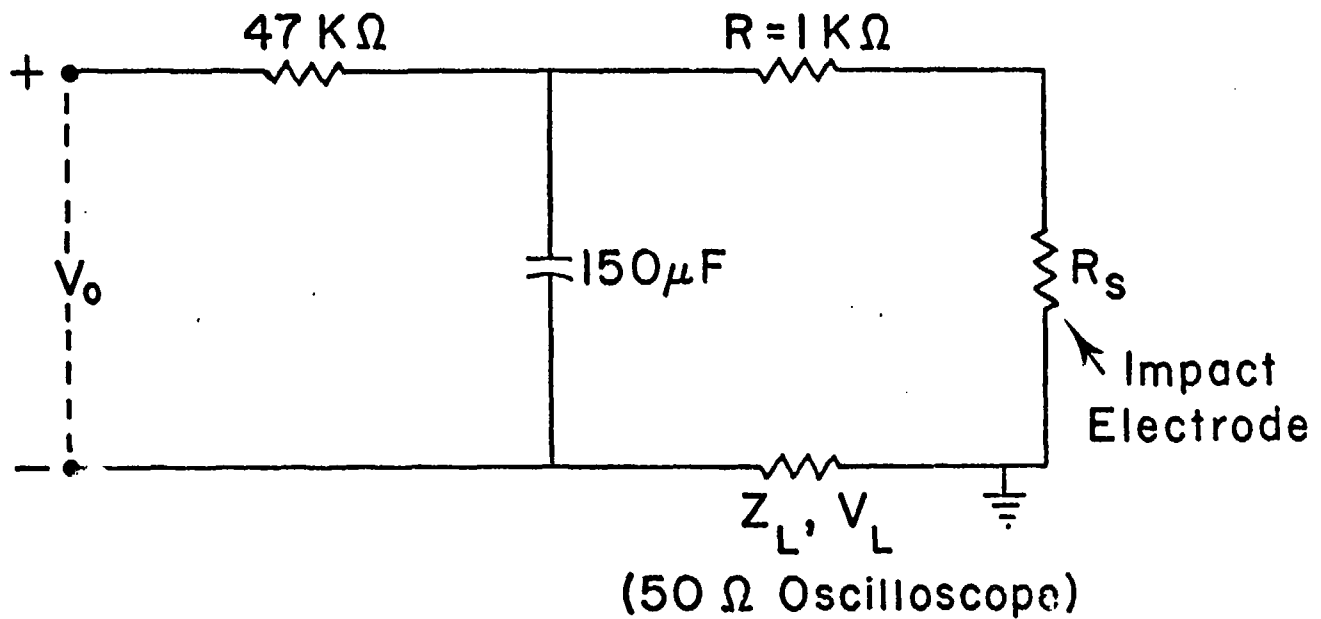


Fig. 2

Resistance Measurement Circuit



R_S Kapton sample

V_L voltage measured by oscilloscope

$$R_S = \frac{V_0 Z_L}{V_L} - (R + Z_L)$$

This is of the form

$$R_S = \frac{A}{V_L} + B$$

Fig. 3

capacitance is large enough that the voltage across it is constant to a fraction of a percent for the 10 μ sec duration of an experiment.

Prior to shock wave arrival, the Kapton is an insulator ($\rho \approx 10^{18} \Omega \text{ cm}$).³ Therefore no switch is needed to keep current from flowing before the experiment.

An analysis of the current shows that the resistance is given by

$$R_S = \frac{V_0 Z_L}{V_L} - (R + Z_L) ,$$

where V_0 is the voltage applied to the capacitor, Z_L is the impedance of the oscilloscope, V_L is the voltage measured by the oscilloscope, and R is the series resistor. This expression is of the form

$$R_S = AV^{-1} + B ,$$

where A and B are constants. Before each shot, the sample was replaced in the circuit by a mercury relay and known resistors. The scopes were then calibrated by measuring the deflection given by several known resistors. The values of A and B were then determined with a linear least squares fitting program.

Ring up to Pressure

In this set of experiments, the final pressure in the Kapton is not achieved in a single shock wave passage through the sample. The sample rings up to the final pressure. This is shown in the x - t diagram (Fig. 4) and the Hugoniot diagram (Fig. 5). In Fig. 4 a shock wave is produced in the impactor and in the copper buffer at impact. The shock in the buffer travels to the copper-Kapton interface where a wave enters the Kapton and a wave is reflected back into the buffer. The wave in the Kapton travels to the Kapton-copper interface where a wave is reflected back into the Kapton and a wave is transmitted into the copper. The reflected wave travels back to the copper buffer interface where a wave is transmitted into the buffer and a wave is reflected back into the Kapton. This process continues at the interfaces until the Kapton has rung up to the final

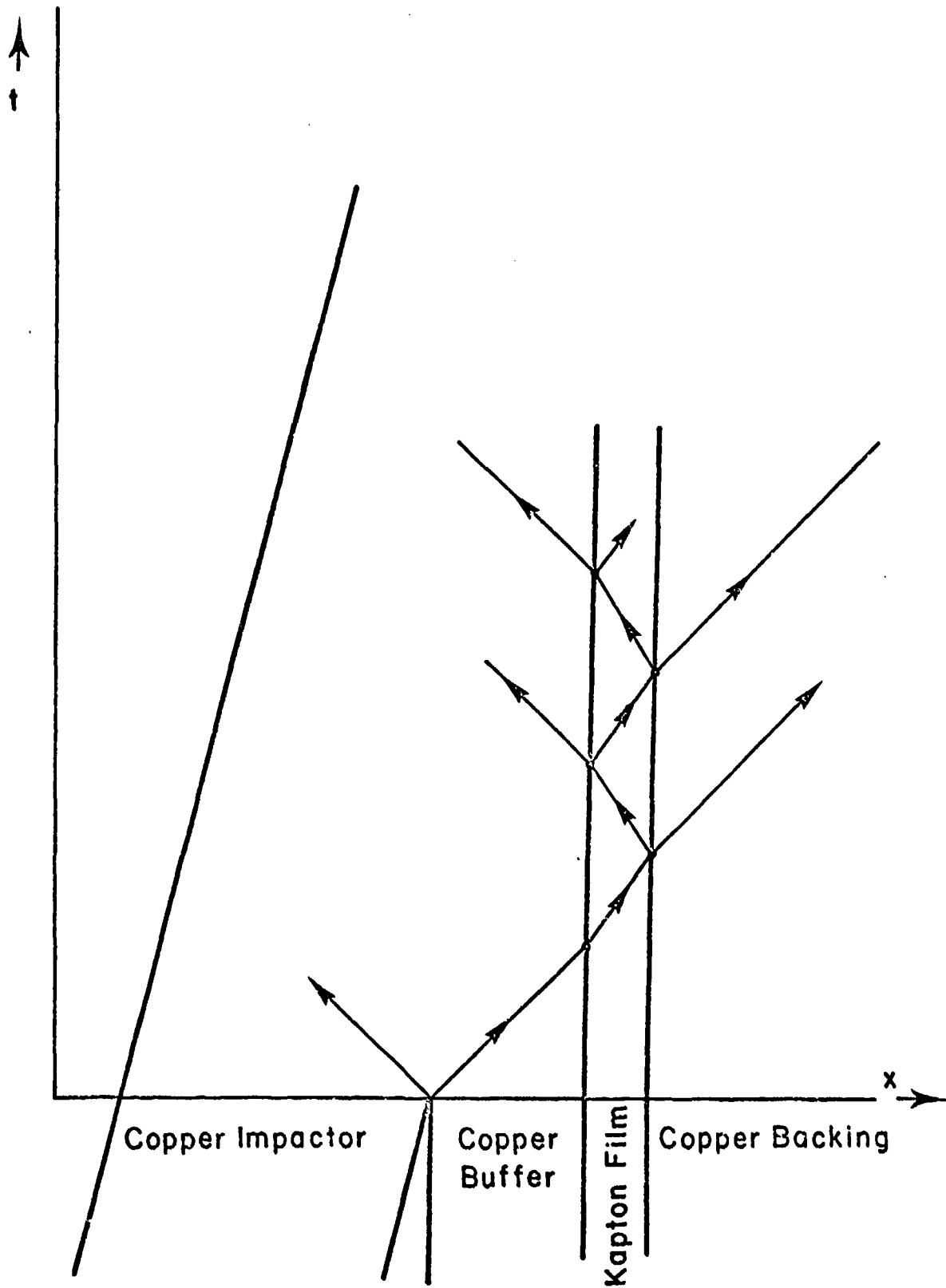


Fig. 4

x-t diagram for Kapton compressed between two copper plates

Kapton Ringing Up Between Copper Electrodes

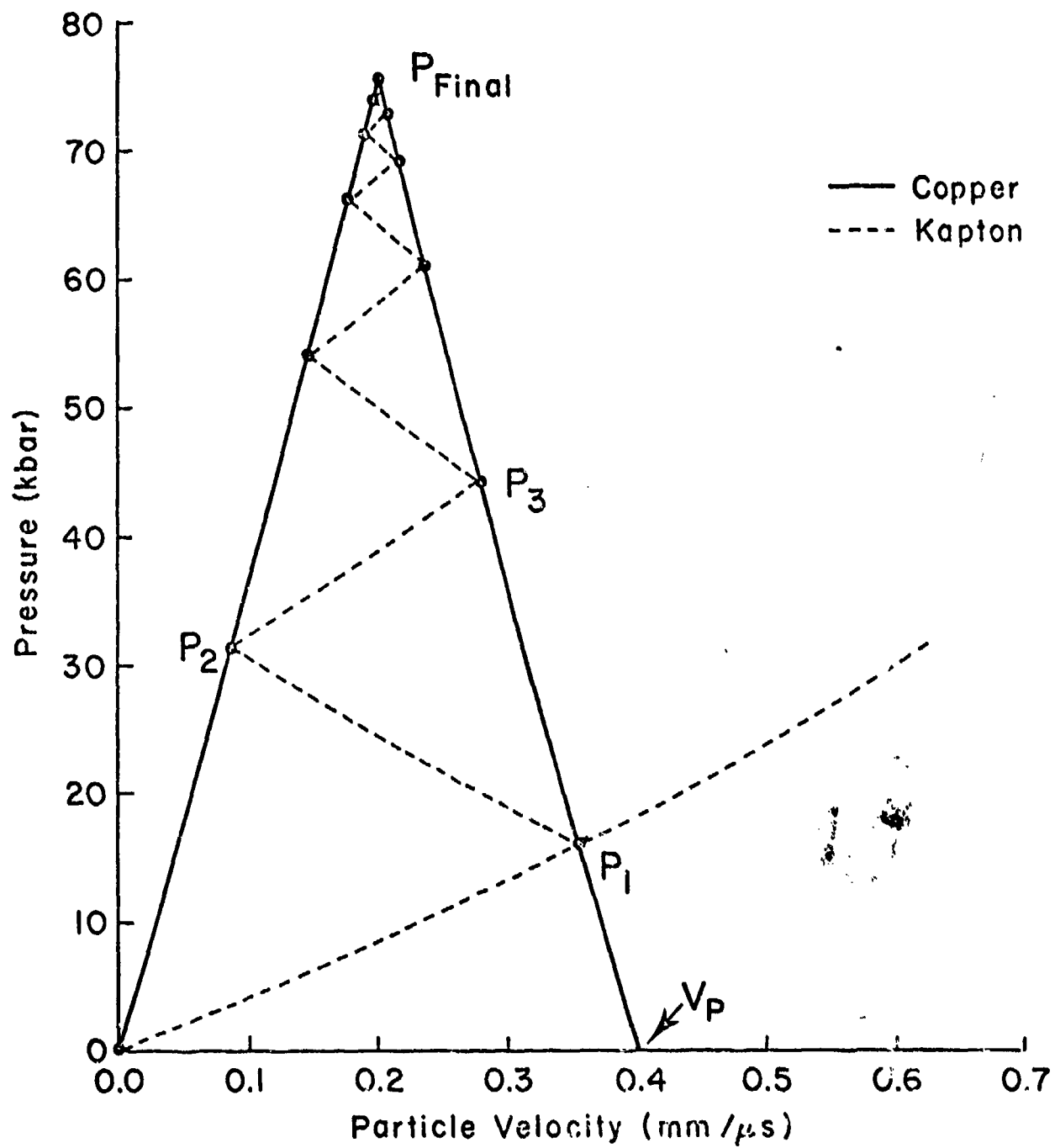


Fig. 5

pressure. The final pressure is that of the copper-copper impact. This process is also shown in Fig. 5, which is drawn to scale. Each shock passage through the Kapton increases the pressure by a smaller amount until a final value is reached.

To get the P,u states in the sample as it rings up we use the following Hugoniot of copper and Kapton.

$$P(\text{kbar}) = 351.8420 u + 132.9677 u^2 \quad \text{copper}^2$$

$$P(\text{kbar}) = 37.6124 u + 20.9272 u^2 \quad \text{Kapton}^1 (U_p \text{ from } 0.6 \text{ to } 2.2 \text{ mm}/\mu\text{s})$$

State 1 (P_1, u_1) is the intersection of forward facing (FF) Kapton Hugoniot and the backward facing (BF) copper Hugoniot that goes through $P = 0, u = \text{projectile velocity}, V_p$. State 2 (P_2, u_2) is the intersection of the BF Kapton Hugoniot that goes through P_1, u_1 and the FF copper Hugoniot through $P = 0, u = 0$. State 3 (P_3, u_3) is the intersection of the FF Kapton Hugoniot through P_2, u_2 and the BF copper Hugoniot through $P = 0, u_p = V_p$.

We continue this process for each reflection at the Kapton-copper interfaces. About 7 shock passages are necessary to bring the Kapton up to 90% of its final pressure. This does put a limit on the response time of the measurements since it takes about 40 to 150 nsec for the Kapton to reach its final pressure. However, we can obtain higher pressures than we could in a single copper on Kapton impact.

Resistivity

We want to obtain the resistivity ρ of a Kapton sample from the measured resistance R. It is given by

$$\rho = \frac{RA}{d}$$

where A is the electrode area and d is the final thickness of the shock compressed sample (see Fig. 6).

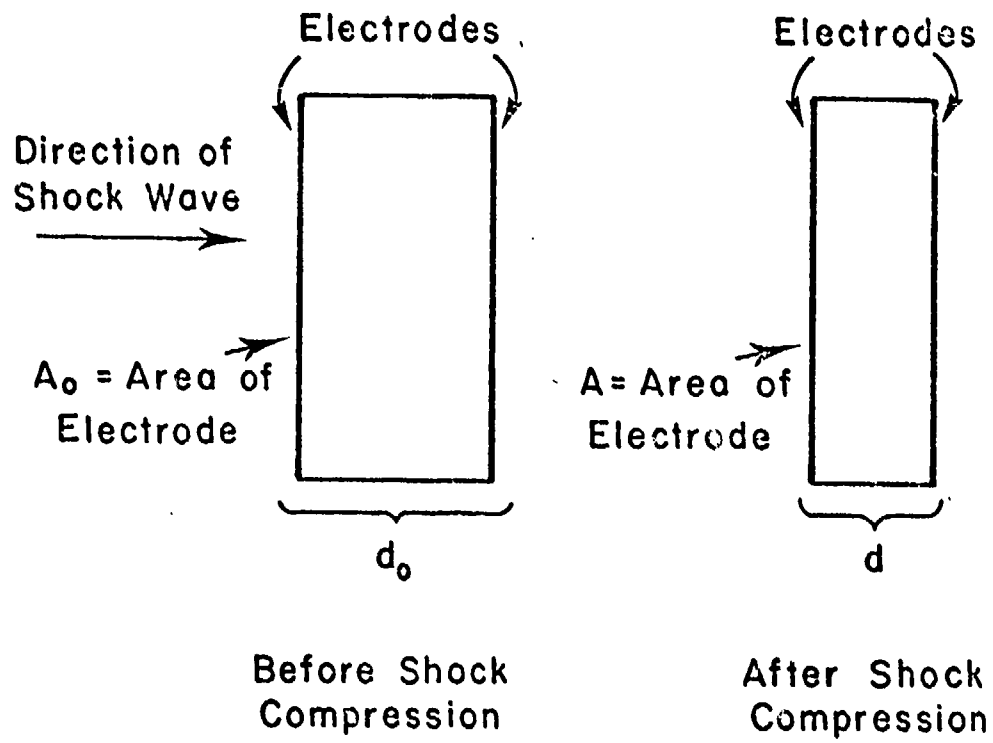


Fig. 6

Uniaxial compression of a Kapton element

We have measured the initial values A_0 and d_0 and must calculate A and d . The initial density of the Kapton, ρ_0^* , is given by

$$\rho_0^* = \frac{m}{A_0 d_0}$$

and the density after shock compression, ρ^* , is given by

$$\rho^* = \frac{m}{Ad}$$

where m is the mass of the sample. Therefore

$$\frac{\rho^*}{\rho_0^*} = \frac{A_0 d_0}{Ad}$$

Since the sample has been compressed uniaxially by the shock wave, A is equal to A_0 , and we have

$$d = \frac{d_0 \rho_0^*}{\rho^*}$$

We can now use the mass and momentum jump conditions

$$\frac{\rho_0^*}{\rho^*} = 1 - \frac{u - u_0}{U - u_0}$$

$$P - P_0 = 10\rho_0^*(U - u_0)(u - u_0)$$

where P_0 and P are the initial and final Kapton pressures in kbar, u_0 and u are the initial and final particle velocities in mm/ μ s, and U is the shock speed in mm/ μ s. By combining these two equations, we obtain

$$\frac{1}{\rho^*} = \frac{1}{\rho_0^*} - \frac{10(u - u_0)^2}{(P - P_0)}$$

This expression gives us the final density of a material that has been compressed by a single shock. In our case, the Kapton rings up to pressure. We go from u_0, P_0, ρ_0^* to u_1, P_1, ρ_1^* to $u_2, P_2, \rho_2^* \dots$ to u_n, P_n, ρ_n^* . Therefore we have

$$\frac{1}{\rho_1^*} = \frac{1}{\rho_0^*} - \frac{10(u_1 - u_0)^2}{(P_1 - P_0)}$$

$$\frac{1}{\rho_2^*} = \frac{1}{\rho_1^*} - \frac{10(u_2 - u_1)^2}{(P_2 - P_1)}$$

$$\vdots$$

$$\frac{1}{\rho_n^*} = \frac{1}{\rho_{n-1}^*} - \frac{10(u_n - u_{n-1})^2}{(P_n - P_{n-1})}$$

Combining these expressions we get

$$\frac{1}{\rho_n^*} = \frac{1}{\rho_0^*} - 10 \sum_{k=1}^n \frac{(u_k - u_{k-1})^2}{(P_k - P_{k-1})}$$

where ρ^* is in g/cm^3 , u is in $\text{mm}/\mu\text{s}$ and P is in kbars.

EXPERIMENTAL RESULTS

The results of these shock wave experiments are presented in the Table and Figs. 7 and 8. At the pressures produced in these experiments (40-150 kbar), the resistivity of Kapton drops 11 to 12 orders of magnitude from its initial value of $10^{18} \Omega\text{cm}$.³

Response Time

This drop in resistivity is characterized by two times, t_1 and t_2 (see Figs. 9 and 10). These figures are accurate tracings of two of the shot records. In each of these shots the resistance dropped from its initial value of $10^{18} \Omega\text{cm}$ to an intermediate value in a time t_1 and from this value to its final value in a shorter time t_2 . The resistance remains fairly constant at this final value for 150 to 200 ns.

The additional decrease in resistance from this final value is a result of the copper electrodes punching through the Kapton and shorting out.

Values of t_1 and t_2 for the shots are given in the Table and plotted against pressure in Fig. 7. An estimate of the uncertainty in taking these measurements

KAPTON SHOCK WAVE EXPERIMENTS

Shot #	Kapton Sheet No. and thickness (mils)	V_p^a (mm/ μ s)	Pressure (kbar)	ρ_0^*/ρ^{*b}	t_1^c (ns)	t_2^c (ns)	Final Resistivity (Ω cm)	Ring-up time in Kapton (10 passes) (ns)
79-043	#1, 1.05 mil	0.759	152.7	0.616	74	-	-	39.7
79-045	#1, 1.05 mil	0.612	120.1	0.650	95	-	-	43.9
79-053	#1, 1.05 mil	0.504	97.1	0.680	130	-	-	47.7
79-054	#1, 1.05 mil	0.320	59.7	0.745	188	-	-	57.0
79-055	#1, 1.05 mil	0.218	39.9	0.795	203	93	6.35×10^6	64.7
79-056	#1, 1.05 mil	0.409	77.5	0.711	142	39	4.18×10^6	52.0
79-058	#1, 1.05 mil	0.747	150.0	0.618	60	43	3.75×10^6	40.0
79-059	#2, 1.05 mil	0.595	116.4	0.654	81	42	3.16×10^6	44.4
79-060	#2, 1.05 mil	0.750	150.6	0.618	63	46	3.23×10^6	39.9
79-061	#2, 1.05 mil	0.497	95.6	0.682	-	-	3.32×10^6	48.0
80-002	#2, 1.05 mil	0.215	39.4	0.797	198	55	5.18×10^6	65.0
80-003	#2, 3.05 mil	0.405	76.7	0.712	136	60	1.89×10^6	151.5
80-004	#2, 3.05 mil	0.598	117.1	0.653	84	63	1.725×10^6	128.7

Copper $P(\text{kbar}) = (10)(8.930)(3.940 + 1.489u_p)(u_p)$

Kapton $P(\text{kbar}) = (10)(1.414)(2.66 + 1.48u_p)(u_p)$

- a. Projectile velocity
 b. Kapton density ratio
 c. t_1 and t_2 are defined in text

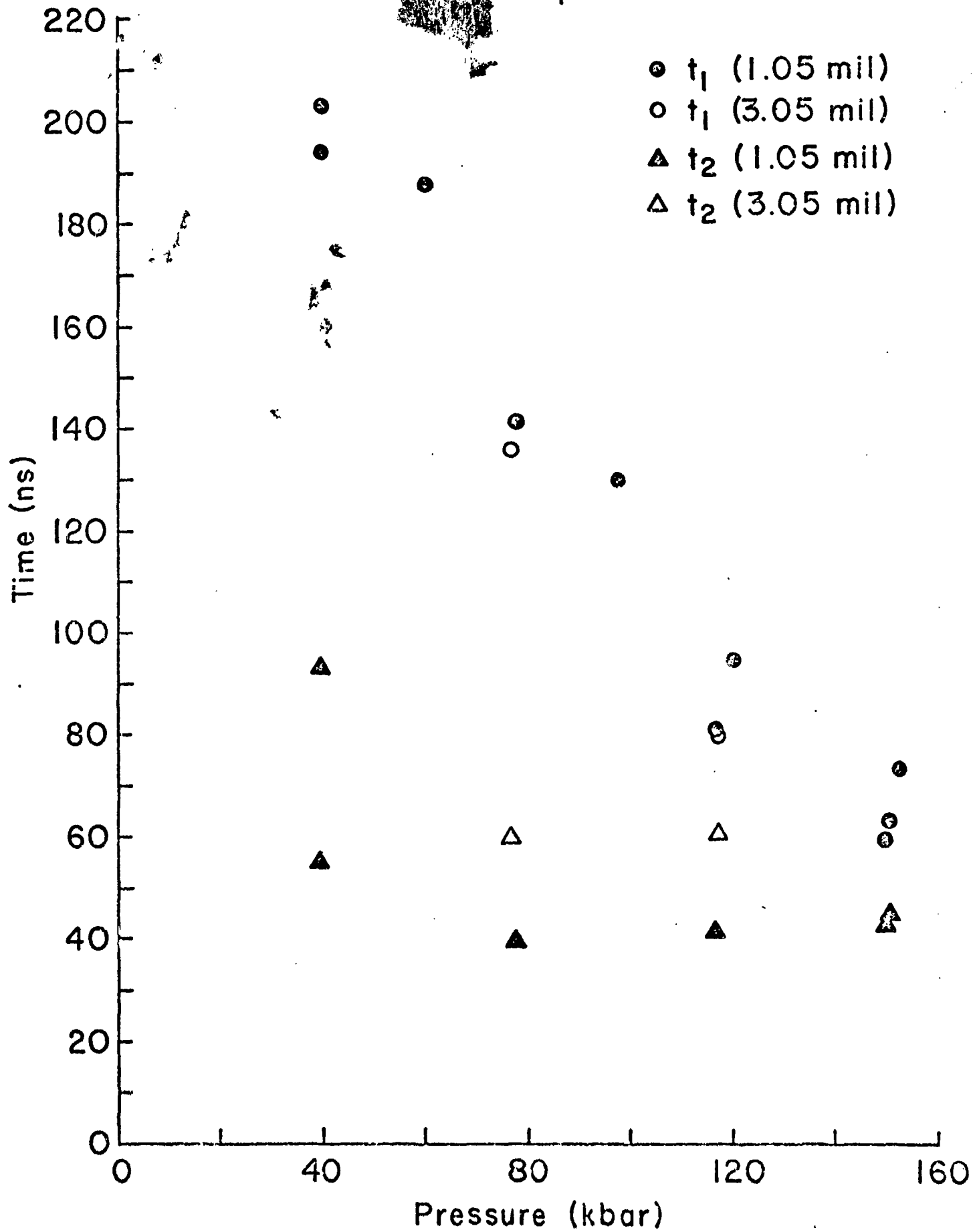
Response Time vs Pressure
for Kapton

Fig. 7

Final Resistivity vs Final Pressure for Kapton

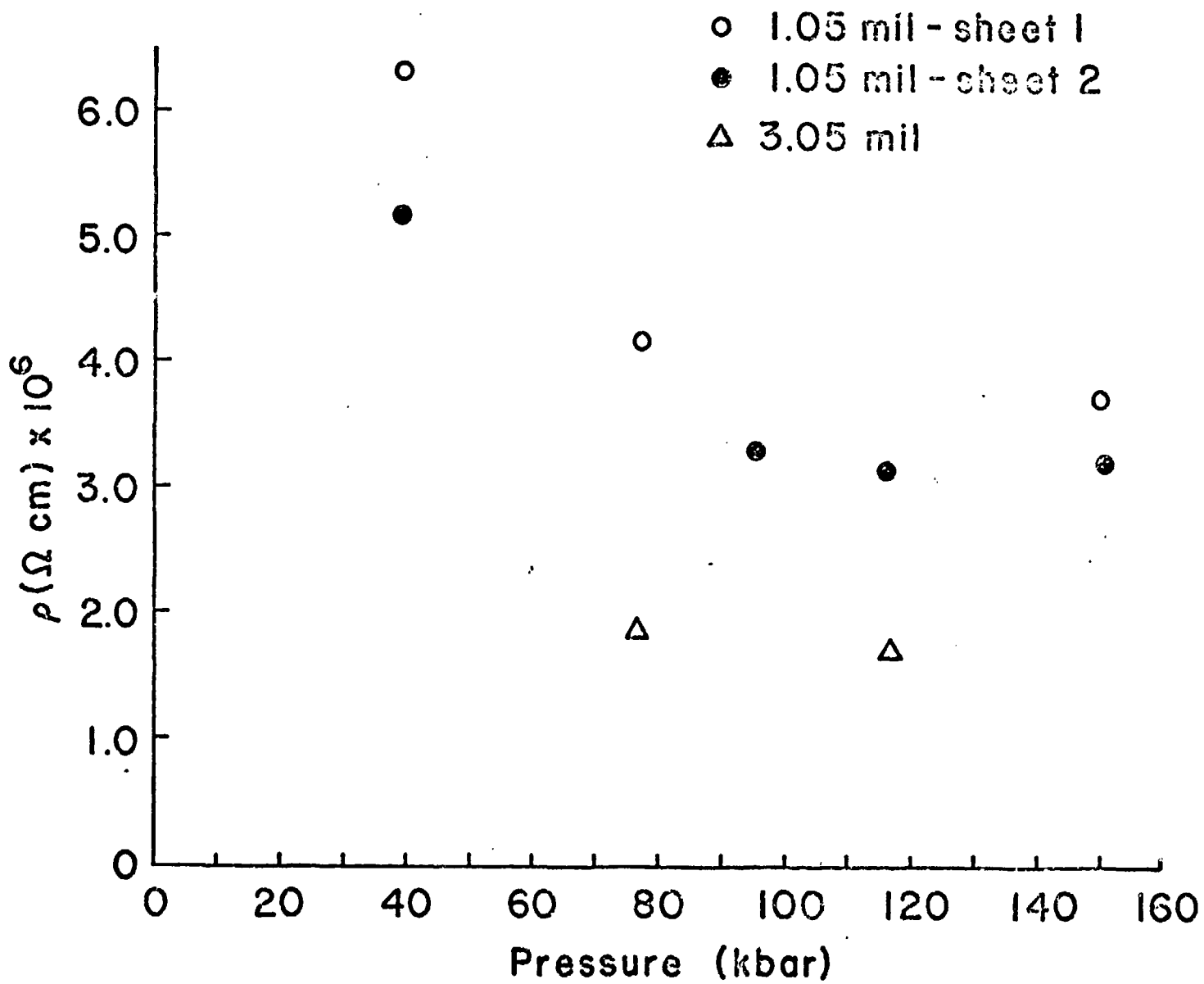


Fig. 8

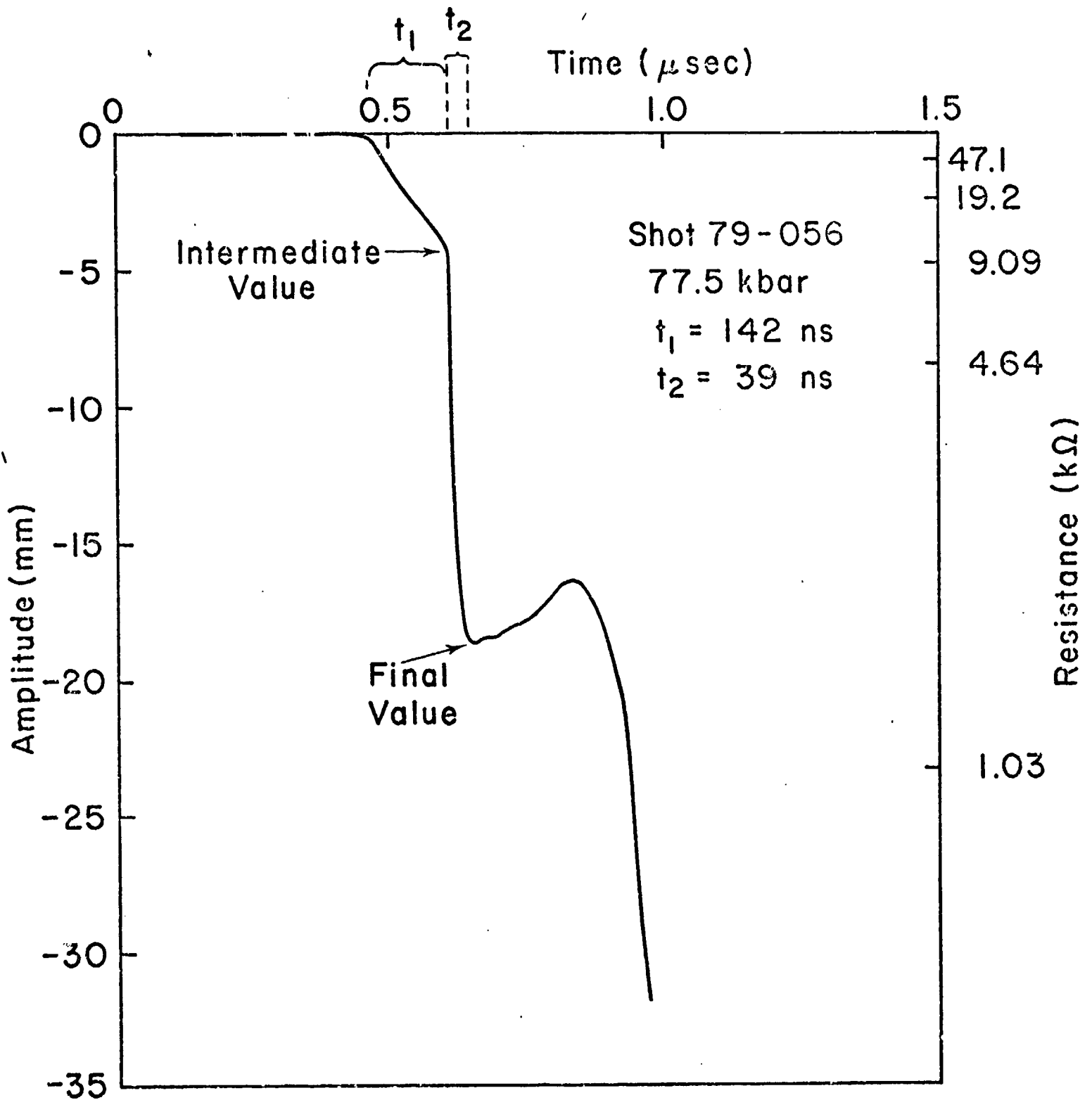


Fig. 9

Tracing of shot record for 1.05 mil Kapton, Shot #79-056

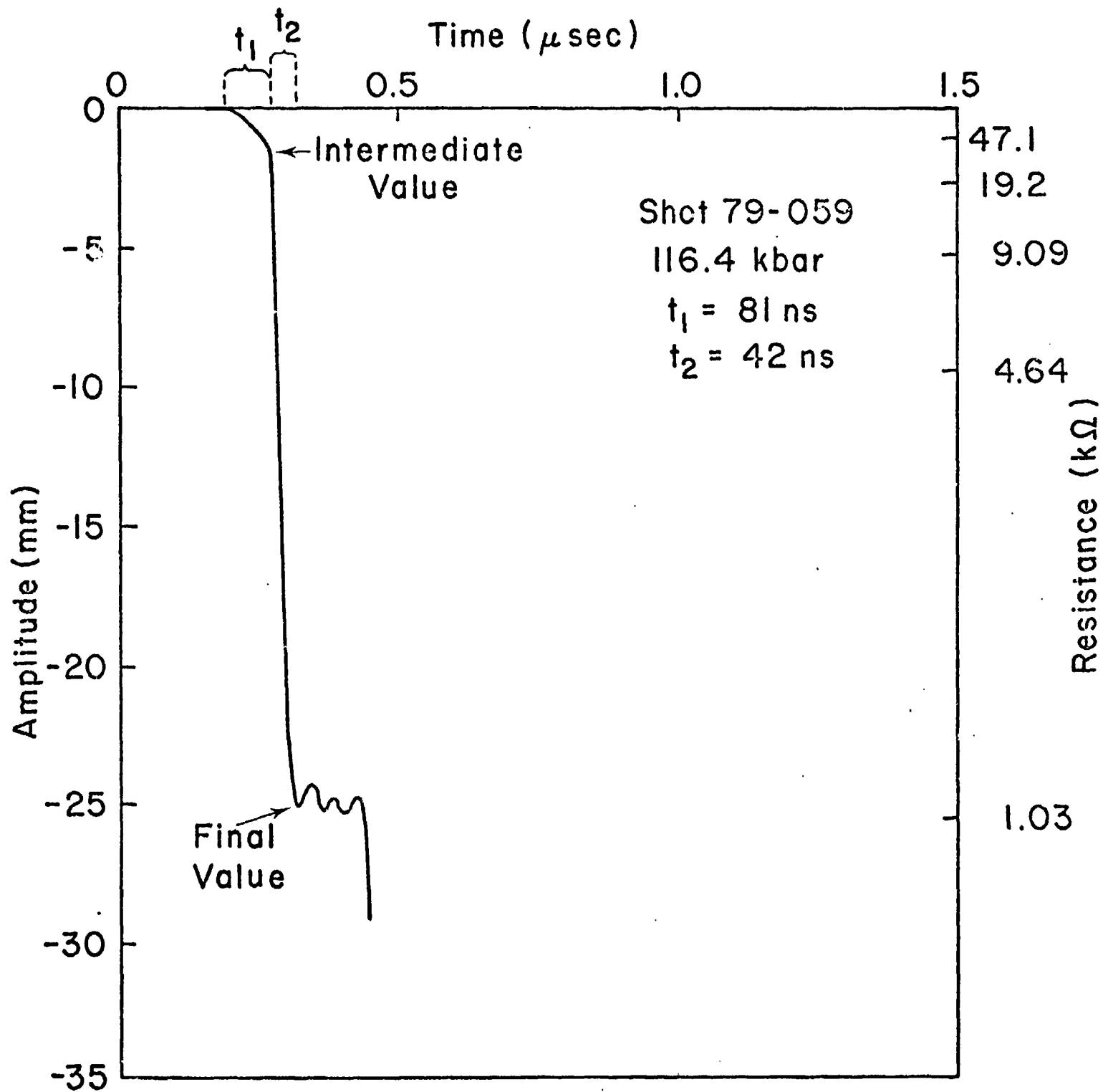


Fig. 10

Tracing of shot record for 1.05 mil Kapton, Shot #79-059

from the scope records is ± 5 to 10 ns. The value of t_1 decreases almost linearly with pressure from a value of about 200 ns at 40 kbar to a value of 60 to 70 ns at 150 kbar. Both the 1.05 mil thick and the 3.05 mil thick samples show this effect.

The value of t_2 is independent of pressure from at least 75 to 150 kbar. The increase in t_2 at 40 kbar is probably due to tilt.

The effects of tilt are shown in Fig. 11. The time t for the gap between the impactor and the active area of the target to close is given by

$$t = \frac{d \tan \theta}{V_p}$$

where d is the diameter of the electrode, θ is the tilt angle and V_p is the projectile velocity. In our experiments, $d = 25.57$ mm and $\theta = 0.25 \times 10^{-3}$ rad is a reasonable value for the maximum tilt giving

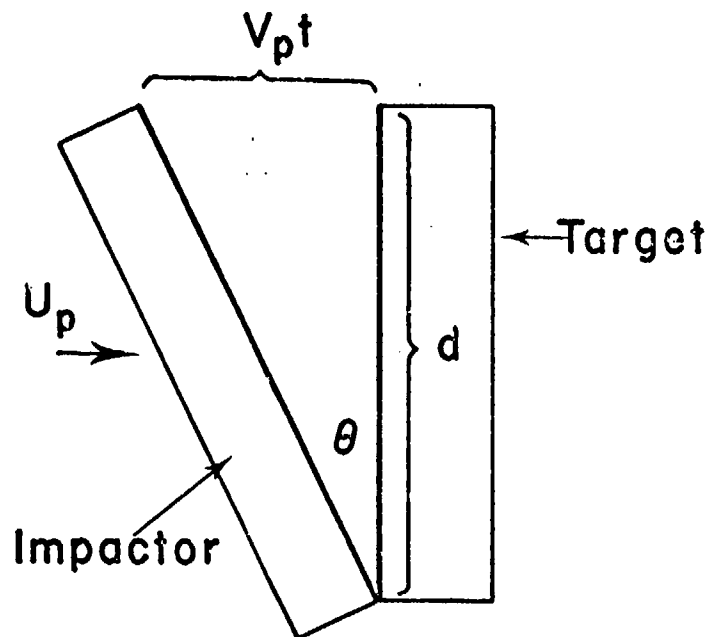
$$t = \frac{6.39 \times 10^{-3}}{V_p}$$

For a projectile velocity of 0.747 mm/ μ s (150 kbar) we get $t = 8.6$ ns. Since this time is of the same order as the measurement uncertainty on the scope traces, we will not see much of an effect of tilt at the higher pressures. However, for a projectile velocity of 0.218 mm/ μ s (39.9 kbar) we get $t = 29$ ns. If we have bad tilt at these pressures, we will measure a larger t_1 and t_2 due to tilt. In principle, the tilt can be measured in each shot and a correction applied, but in practice, the measurements are not that reliable. It is very difficult to insure that the tilt pins short at impact. They can short through small amounts of gas that are compressed between the projectile and the pin, making the measurement useless.

We now want to consider the time it takes for a sample to ring up to pressure. The time τ it takes for a shock wave to go through the sample is given by

$$\tau = \frac{d_i}{V_s}$$

Tilt Calculation



θ = tilt angle

V_{pt} = projectile velocity

d = diameter of active area
of sample

t = time for gap to close

$$t = \frac{d \tan \theta}{V_p}$$

Fig. 11

where d_i is the thickness of the sample prior to the shock wave passage and V_s is the shock speed measured with respect to the material in front of it. We now use the momentum jump condition

$$P_f - P_i = 10 \rho_i^* (V_s) (u_f - u_i)$$

where P_i is the pressure in front of the shock wave, P_f is the pressure behind the shock wave (both in kbar), V_s is the shock speed in mm/ μ s, ρ_i^* is the density in front of the shock and u_i and u_f are the particle velocities in front of and behind the shock wave. This gives us the following expression for V_s

$$V_s = \frac{P_f - P_i}{10 \rho_i^* (u_f - u_i)}$$

Substituting this into the expression for τ gives

$$\tau = \frac{10 \rho_i^* d_i |u_f - u_i|}{(P_f - P_i)}$$

For the first shock through the material $P_i = P_0 = 0$, $P_f = P_1$, $u_i = u_0 = 0$, $u_f = u_1$, $\rho_i^* = \rho_0^*$, and $d_i = d_0$,

$$\tau_1 = \frac{10 \rho_0^* d_0 u_1}{P_1}$$

For the second shock through the material $P_i = P_1$, $P_f = P_2$, $u_i = u_1$, $u_f = u_2$, $\rho_i^* = \rho_1^*$, and $d_i = d_0 \rho_0^* / \rho_1^*$. Therefore

$$\tau_2 = \frac{10 d_0 \rho_0^* |u_2 - u_1|}{P_2 - P_1}$$

For the n th passage through the material we have

$$\tau_n = \frac{10 d_0 \rho_0^* |u_n - u_{n-1}|}{P_n - P_{n-1}}$$

The total time T_n that it takes in a sample to come up to a pressure P_n is thus given by

$$\tau_n = \sum_{i=1}^n \tau_i = 10 d_0 \rho_0 * \sum_{i=1}^n \frac{|u_i - u_{i-1}|}{P_i - P_{i-1}} .$$

We now have to choose a value for n . If we choose $n = 10$, the sample has come up to about 96% of its final pressure for a shot to 39.9 kbar and 99% of its final pressure for a shot to 150 kbar. For the 1.05 mil samples τ_{10} (at 39.9 kbar) = 64.7 ns and τ_{10} (at 150 kbar) = 40 ns. These times are consistent with the measured values of t_2 for the 1.05 mil thick sample. However, this may be coincidence. If we look at the data for the 3.05 mil samples (shots 80-003 and 80-004) we see that the measured values of t_2 for these shots are only about 1.5 times the t_2 values of 1.05 mil samples shocked to the same pressures, instead of the 2.9 times we would expect from the shock time calculation.

Thus t_1 and t_2 are properties of either the bulk material or the surfaces. The fact that the values of t_2 for the 3.05 mil thick samples are 1.5 times longer than those for the 1.05 mil samples indicate that the shock-up time is influencing the measurement of t_2 .

Resistivity Data

The final resistivity of Kapton decreases with pressure (see Fig. 8 and Table). Two different sheets of Kapton were used for the 1.05 mil shots. The resistivities of the samples from sheet 2 were lower than those from sheet 1. In addition, the resistivity of the 3.05 mil samples were even lower than those of the 1.05 mil samples. This can be explained by surface effects. Since we have no knowledge of the resistance between the vapor deposited electrodes and the sample, we have assumed that this resistance is zero in our calculation of the resistivity from the resistance. We have also assumed that the Kapton film is homogeneous. However, material on the surface is possibly different from that in the interior and independent of the thickness of the film. A substantial resistance due to these surface effects would give us a smaller calculated resistivity for the thicker samples.

Graham¹ has done polarization studies on poly (pyromellitimide), PPMI, which is a bulk form of Kapton. He has noted three different response regions which he calls (1) a subthreshold region, (2) a strong-generation region, and (3) a saturation region.

He believes that the subthreshold region applies for compressions of less than 10 or 15%. The strong-generation region occurs for compressions of about 15 to 30%. In this region, the polarization is a strong function of pressure. The saturation region occurs for compressions greater than 30 to 40%.

Since Graham believes that the observed polarization in this material is due to mechanically induced bond scission (and therefore a production of charge carriers) the resistivity should be characterized by the same response regions.

Our data have been taken between 39.4 kbar (~20% compression) and 152.7 kbar (~38% compression). An examination of our data shows that the resistivity decreases rapidly with pressure up to about 95.6 kbar (~32% compression) and then remains fairly constant to our highest pressure of 152.7 kbar. This is consistent with Graham's work.

REFERENCES

1. R. A. Graham, J. Phys. Chem. 83 (23), 3048 (1979).
2. "Selected Hugoniot," Los Alamos Scientific Laboratory Report LA-4167-MS, 1969.
3. Dupont, Bulletin H-4.